NASA TECHNICAL MEMORANDUM

NASA TM X-2526

NASA TM X-2526

ENGINE INVESTIGATION OF AN AIR-COOLED TURBINE ROTOR BLADE INCORPORATING IMPINGEMENT-COOLED LEADING EDGE, CHORDWISE PASSAGES, AND A SLOTTED TRAILING EDGE

by Robert P. Dengler, Frederick C. Yeh, James W. Gauntner, and Gerald E. Fallon

Lewis Research Center
Cleveland, Ohio 44135

NATIONAL AERONAUTICS AND SPACE ADMINISTRATION • WASHINGTON, D. C. • APRIL 1972

1. Report No.	2. Government Accession No.	3. Recipient's Catalog No.
NASA TM X-2526		

4. Title and Subtitle	5. Report Date
ENGINE INVESTIGATION OF AN AIR-COOLED TURBINE ROTOR BLADE INCORPORATING IMPINGEMENT-COOLED LEADING EDGE, CHORDWISE PASSAGES, AND A SLOTTED TRAILING EDGE	April 1972
	6. Performing Organization Code

7. Author(s)	8. Performing Organization Report No.
Robert P. Dengler, Frederick C. Yeh, James W. Gauntner, and Gerald E. Fallon	E-6450
	10. Work Unit No. 764-74

9. Performing Organization Name and Address	11. Contract or Grant No.
Lewis Research Center National Aeronautics and Space Administration Cleveland, Ohio 44135	
	13. Type of Report and Period Covered Technical Memorandum

12. Sponsoring Agency Name and Address	14. Sponsoring Agency Code
National Aeronautics and Space Administration Washington, D.C. 20546	

15. Supplementary Notes

16. Abstract

Experimental temperatures are presented for an air-cooled turbine rotor blade tested in an engine. The data were obtained for turbine stator inlet temperatures from 1367 to 1644 K (2000° to 2500° F) and for turbine-inlet gas pressures from 22 to 32 newtons per square centimeter (32 to 46 psia). Average and local blade heat-transfer data are correlated. Potential allowable increases in gas temperature are also discussed.

17. Key Words (Suggested by Author(s))	18. Distribution Statement
Turbine blade cooling Heat-transfer characteristics Turbojet engine tests	Unclassified - unlimited

19. Security Classif. (of this report)	20. Security Classif. (of this page)	21. No. of Pages	22. Price*
Unclassified	Unclassified	44	$3.00

* For sale by the National Technical Information Service, Springfield, Virginia 22151

ENGINE INVESTIGATION OF AN AIR-COOLED TURBINE ROTOR BLADE INCORPORATING IMPINGEMENT-COOLED LEADING EDGE, CHORDWISE PASSAGES, AND A SLOTTED TRAILING EDGE

by Robert P. Dengler, Frederick C. Yeh, James W. Gauntner, and Gerald E. Fallon

Lewis Research Center

SUMMARY

An experimental investigation of the heat-transfer characteristics of an air-cooled turbine rotor blade incorporating an impingement-cooled leading edge, chordwise passages in the midchord regions, and a slotted trailing edge for expelling the coolant is discussed. Engine test operation included stator-inlet gas temperatures and pressures as high as 1657 K (2523° F) and 32 newtons per square centimeter (46 psia), respectively, and cooling air temperatures as high as 699 K (798° F) over a range of coolant flow ratios from about 0.017 to 0.130.

Average and local blade heat-transfer data are correlated using a temperature difference ratio φ as a function of the coolant-to-gas flow ratio w_c/w_g. This correlation is recommended because it has a minimum of data scatter, is easy to apply, and can be used for design calculations where the design conditions are similar to those presented in this report. A comparison of average measured blade temperatures and those calculated using the φ correlation equations generated from the data show agreement within ±2.5 percent. Because the original blade design exhibited large temperature gradients and a hot leading edge, a design study was made of a revised internal fin arrangement and leading-edge impingement cooling configuration.

This study indicates that the cooling configuration modifications will provide acceptable maximum leading edge temperatures and temperature gradients that are somewhat reduced for the range of conditions covered in the experimental tests.

INTRODUCTION

The purposes of this report are (1) to present experimental heat-transfer data for an air-cooled turbine rotor blade, (2) to substantiate a method of correlating that data, and (3) to evaluate and improve the design of the rotor blade.

Materials currently in use for the fabrication of turbine vanes and blades are being pushed to their temperature limits based on the required stress level in the turbine. An increase in turbojet engine output can be achieved, however, through efficient cooling of the turbine components, which will permit operation at elevated gas temperatures. Because turbine blades are subjected to both high gas temperatures and high centrifugal loads, they are the most critical components of the turbine assembly. In order to design air-cooled turbine blades for future advanced engines, it is necessary to accurately estimate airfoil blade metal temperatures for a given set of engine operating conditions. In addition to efficiently reducing blade metal temperatures, the blade cooling should not cause extreme temperature gradients as this would greatly reduce the blade life. Ideally, blade airfoil temperatures should be predicted analytically. Attempts at developing adequate analytical prediction methods are in progress; however, until such methods become perfected, empirical correlations like those developed herein will be required for estimating airfoil temperatures. Successful correlation of data taken over a limited range of variables should permit the estimation of airfoil temperatures for any similar set of operating conditons, thereby eliminating a vast amount of testing.

Various methods for either calculating or correlating airfoil temperature data are presented in references 1 and 2. Modifications of the method used in reference 1 were made in reference 3 to correlate experimental turbine vane temperatures. The present report represents another attempt at determining the best method of correlating heat-transfer data. The data correlation methods for the turbine blade reported herein closely follow those in reference 3.

A modified high-pressure spool section of a turbojet engine was used to conduct the heat-transfer tests reported herein. Turbine blade temperatures were obtained for cooling-air-to-gas flow ratios from 0.017 to 0.130, at turbine stator-inlet temperatures from about 1367 to 1644 K (2000° to 2500° F). At these temperatures, the turbine-inlet gas pressures varied from a minimum of 22 to a maximum of 32 newtons per square centimeter (32 and 46 psia, respectively), and the turbine-inlet gas flow rate varied from about 23 to 36 kilograms per second (50 to 80 lbm/sec).

APPARATUS

Engine Facility

The high-pressure section of a conventional two-spool turbojet engine (military designation, J-75) was modified to provide a test bed for obtaining air-cooled turbine blade heat-transfer data. The entire test facility, including the engine, test cell, instrumentation systems, and data acquistion systems, is described in detail in reference 4. A photograph of this research engine is shown in figure 1 of this report.

The modified engine contains a single-stage turbine with provisions to supply cooling air to the turbine stator vanes and rotor blades from external sources. The turbine rotor contains 76 blades. Five adjacent positions in the turbine rotor accept blades of a particular cooling configuration to form a rotating cascade, while the remaining 71 positions in the rotor accommodate air-cooled workhorse blades. It is intended that the same so-called workhorse blades be used in the turbine rotor while various test-blade configurations are investigated for determining their cooling performance. Hereinafter, the cascade of five adjacent blades shall be indentified as test blades, and the remaining 71 workhorse blades shall be identified as slave blades. Figure 2 is a photograph of the downstream side of the turbine rotor with all test and slave blades installed. The nominal blade chord and span dimensions are 4.1 and 10.2 centimeters (1.6 and 4.0 in.), respectively. For all testing, cooling air was supplied to the turbine blades from external sources rather than using bleed-off air from the engine compressor. This procedure allows much greater flexibility in supplying air over a range of temperatures and coolant flow rates. In addition, a dual air cooling arrangement (described in ref. 4) is used so that the temperature and flow rate of the cooling air supplied to the test blades and slave blades can be controlled and metered from independent external sources. Figure 3 represents the hot section of the research engine and illustrates the separate paths for external cooling air flow to both the turbine slave blades and the test blades. This arrangement permits the overcooling of the slave blades with respect to the test blades to promote extended slave blade life, since these blades are to be subsequently used with other groups of research blades. In addition, this approach permits the fabrication of only a small number of test blades, thus keeping the cost of providing relatively complex test hardware to a reasonable minimum.

The schematic illustration of figure 4 defines the flow path for cooling air supplied to the test blades. The transfer of cooling air from a stationary manifold within the engine tailcone to the rear side of the rotating turbine rotor disk is accomplished with the use of a balanced-pressure labyrinth seal system. This seal system is described in detail in references 4 and 5.

Test Blade

The blade of this report was designed to operate at a gas temperature relative to the blade of 1533 K (2300° F), a coolant inlet temperature of 922 K (1200° F), and a coolant-to-gas flow ratio of 0.03 with a resulting hotspot metal temperature of 1255 K (1800° F). For a normal amount of dilution from the stator row, the relative gas temperature of 1533 K (2300° F) is approximately equal to 9/10 of the stator inlet gas temperature of 1703 K (2607° F).

Blade description. - The blade design incorporates impingement cooling, multiple small chordwise passages, and a slotted trailing edge. Figure 5 illustrates the rather complicated cooling design incorporated in this blade, and also provides some pertinent dimensions.

Cooling air entering at the base of the blade initially flows into a central cavity of the airfoil. This feature provides for the distribution of cooling air at a relatively constant temperature from base to tip. From here the air flows through a row of 0.084-centimeter (0.033-in.) diameter holes with 0.13-centimeter (0.05-in.) center to center spacing in a sheet metal partition.

These holes act as orifices, and the coolant flowing through them provides impingement cooling for the leading edge. The distance of the holes from the inner surface of the leading edge is 0.356 centimeter (0.140 in.). This places the row of impingement holes eight equivalent slot widths from the inner surface of the leading edge. (The equivalent slot width is defined as the area of one impingement hole divided by the center-to-center distance between two adjacent holes.)

After impinging the internal surface of the blade leading edge, the cooling air subsequently splits into two paths and flows rearward through chordwise passages of 0.076- by 0.076-centimeter (0.030- by 0.030-in.) cross section on both the pressure and suction halves of the blade. There are 50 such passages on the pressure (concave) side, and 80 passages on the suction (convex) side. For the given blade geometry, calculations showed that 60 percent of the total coolant flowed through the chordwise passages on the suction side of the blade, and the remaining 40 percent flowed through the pressure side of the blade. Coolant exiting from the finned passages flows into a common plenum area before exiting through a split trailing edge.

For structural reasons, the split trailing edge design has intermittently spaced lands that join the suction and pressure sides of the blade. These lands are of varying length to allow for a preferential coolant flow distribution favoring the base region of the blade airfoil. As shown in figure 5, there are three different sized split trailing edge slots from which the coolant exits.

Blade fabrication. - A normal procedure for porducing commercial or production turbine blade hardware is to use casting processes. Because this rather complex

design would undoubtedly require a lengthy development time for fabrication, more expedient and economical means were explored for producing a small number of test blades for research purposes. The method of fabrication used machining and joining techniques such as electric discharge machining, brazing, and electron beam welding. Figure 6 illustrates the blade in various stages of fabrication. In general, fabrication of these blades was achieved by first electric discharge machining the chordwise fins into solid blade casting of Udimet 700, a nickel base superalloy. Other materials may have better stress-rupture properties, but for research purposes Udimet 700, which has somewhat better welding characteristics, was used. A solid blade casting was used in the machining of each integral base airfoil blade half for both the suction and pressure sides. The parting line for the blade halves was along the blade leading and trailing edge and continued down through the blade base. Pieces of 0.0180-centimeter (0.007-in.) thick L-605 sheet material were brazed to the machined fins to form the chordwise passages for each respective blade half. A 0.051-centimeter (0.020-in.) L-605 bulkhead sheet with the array of impingement holes was also brazed to one blade half. A second brazing cycle was required to complete the attachment of the impingement bulkhead to the other blade half and also at the end of the chordwise passages where the sheet metal pieces meet, to prevent leakage of the cooling air from the central cavity. The blade halves were then electron beam welded along the leading edge and along the lands at the trailing edge. Figure 7 shows a blade assembly after completion of all fabrication operations.

The fabrication techniques were used for expediency. Advanced fabrication methods are being developed for production hardware. Two methods currently being investigated - gas pressure welding and activated diffusion brazing - show promising results. Chordwise finned blades with airfoil span lengths and chord widths of 5.08 centimeters (2.0 in.) and 3.6 centimeters (1.4 in.), respectively, have been successfully fabricated using the activated diffusion brazing process. Preliminary results of these investigations are reported in reference 6.

INSTRUMENTATION

Engine

The research engine was instrumented extensively to provide information on engine operation and environmental conditions in the turbine test section. This instrumentation consisted primarily of thermocouples and pressure taps. Measurements from this instrumentation were recorded by a central data recording system and, in addition,

some of these measurements were also monitored in the facility control room for operational purposes and for setting and checking test points. The general operational instrumentation and the central data recording system are described in more detail in reference 4. The research instrumentation provided measurements of gas stream conditions, cooling-air flow conditions, and test-blade metal temperatures. The instrumentation for determining gas flow and cooling-air flow conditions is also discussed in reference 4. Eight thermocouple probes are located at various circumferential positions at the exit of the combustors for obtaining the stator-inlet gas temperatures. Each of these probes was actuated radially to provide temperatures at nine similar spanwise locations to determine a representative average stator-inlet temperature. The turbine rotor test-blade cooling-air flow rate was measured upstream of the pressure-balanced labyrinth seal through the use of a venturi. The temperature and static pressure of the cooling air was also measured in the test-blade cooling-air annular chamber immediately before the coolant enters the rotating turbine disk. This is the last place in the test-blade cooling-air flow path that the pressure was measured. Thermocouples were installed to measure the temperature of the coolant just before it entered the test blades.

Blade

The five test blades were instrumented with 23 Chromel-Alumel thermocouple assemblies imbedded in the airfoil walls in order to obtain local metal temperatures and to determine the test-blade chordwise temperature distributions. Figure 8 indicates the relative chordwise and spanwise locations of thermocouples on the five adjacent test blades and their relative position when installed in the turbine rotor. Table I lists the actual surface distance x, and the nondimensional surface distance x/L_p or x/L_s as measured from the extreme blade leading edge to the measuring location for all blade wall thermocouples at their respective blade span positions. All symbols are defined in appendix A. As noted, the thermocouples were located at three different spanwise sections namely, 1.27, 3.81, and 5.08 centimeters (0.5, 1.5, and 2.0 in.) above the platform, and at seven various chordwise positions around the blade periphery. The majority of the thermocouples (15) were concentrated at the 3.81-centimeter (1.5-in.) span location; four each were located at the other two spanwise section locations. The structural integrity of the blade assembly was carefully considered when locations for thermocouples were selected. In particular, the extreme leading edge (where the two blade halves are joined through an electron beam welding process) was therefore purposely avoided. The thickness of the tapered blade shell also limits the placement of thermocouples to a span position at a distance of 5.08 centimeters (2.0 in.) or less

from the blade base platform. The blade airfoil shell thickness decreases from about 0.152 centimeter (0.060 in.) at the blade base region to about 0.076 centimeter (0.030 in.) at the blade tip. Allowing for structural considerations and because of physical limitations, the maximum number of thermocouples installed on any individual test blade was five.

Swaged thermocouple assemblies were installed in radial grooves that had been machined in the blade surface. These assemblies consisted of 0.01-centimeter (0.004-in.) diameter Chromel/Alumel wires with magnesium oxide insulation, which, in turn were contained in an Inconel sheathing. The wires and insulation were then swaged to a final diameter of about 0.051 centimeter (0.020 in.). All thermocouples installed on the blade were of the closed-ball type with the thermocouple junction electrically grounded to the sheath. The quality control for such thermocouple assemblies was maintained by following the rigid procedures and recommendations outlined in reference 7

TEST PROCEDURE

For obtaining the required heat-transfer information of this particular cooled-blade design, the engine was operated over a range of stator-inlet temperatures from 1367 to 1644 K (2000° to 2500° F) with the engine speed varying from about 7300 to 8700 rpm. Three nominal blade cooling-air inlet temperatures were investigated at these engine conditions, with most of the testing being conducted with cooling air at about 380 K (224° F). An individual series of tests was also conducted for cooling air inlet temperatures of approximately 489 and 689 K (420° and 780° F). A series of tests is herein defined as a group of test points made at a constant stator-inlet temperature and constant nominal cooling-air inlet temperature (at blade base). For a given series, a change of coolant flow rate was the primary variable from one run to the next. Since most of the pertinent instrumentation was located near the midspan position, the stator-inlet temperature was established as the average of the measurements at the middle three radial positions for each of the eight actuated thermocouple probes, which is an average of 24 measurements. A summary of pertinent engine operating conditions for each series of runs, along with all blade temperature data, is given in table II. A specific symbol is designated for each series of runs listed in this table and is used to represent respective data in all the figures.

The general engine operating procedure for a given series of tests was to start with a relatively large coolant flow rate (ratio of coolant flow to gas flow) supplied to the test blades. For each successive run in a series of tests, the coolant flow rate to the test

blades was reduced from the coolant flow rate for the previous run. This procedure of reducing the coolant flow in a stepwise manner was continued until a maximum blade metal temperature of 1200 K (1700° F) had been reached. Considering the stress-rupture characteristics of the blade material, the resulting temperature gradients, and the blade fabrication procedures, the 1200 K (1700° F) temperature level was considered the maximum safe operating temperature for the test-blade configuration. After the minimum coolant flow condition was reached, generally two additional runs were made at intermediate coolant flow rates to serve as check points for data taken previously. Usually about eight data points were taken for each series of tests. The coolant-to-gas flow ratio w_c/w_g varied from 0.017 to 0.130.

ANALYSIS METHODS

Correlation Equations

A method for correlating experimental heat-transfer data for a surface cooled by convection was presented in reference 3. The resulting equation is written as

$$Y = K_1\left[\left(\frac{w}{\mu}\right)_g^n \Big/ \left(\frac{w}{\mu}\right)_c^m\right] \tag{1}$$

where

$$Y = \frac{1 - \varphi}{\varphi} \frac{Pr_c^{1/3} k_c}{Pr_g^{1/3} k_g} \tag{2}$$

and

$$\varphi = \frac{T_{g,e} - T_w}{T_{g,e} - T_c} \tag{3}$$

By considering property values constant, a simplification to equation (1) results. It is

$$\frac{1 - \varphi}{\varphi} = K_2\left(\frac{w_g^n}{w_c^m}\right) \tag{4}$$

A further simplification can be achieved by assuming that the exponents m and n are equal. The results of this additional simplification can be obtained by expressing φ as a function of w_c/w_g. Experimental data from this report are discussed using these three correlation methods.

Application to Blade

Application of the preceding correlations will be limited to that section of the blade where the majority of the thermocouples were installed; that is, 3.81 centimeters (1.5 in.) above the blade platform. Individual blade wall temperatures are used for correlations of local data, whereas an integrated average of the measured temperatures at all thermocouple locations at this blade span section is used for correlation of the average blade temperature $\overline{T}_w$.

Equation (3) requires the knowledge of an effective gas temperature and representative coolant temperature. Because the blade coolant passages are relatively small and complex, it was not practical to install cooling-air instrumentation within the blade airfoil. Therefore, the experimental value of T_c in equation (3) was indicated by the thermocouples located at the cooling-air inlet to the blade base (see fig. 4). The value of cooling-air temperature as indicated by these thermocouples $T_{c,b,i}$ was used for correlations based on both average and local blade metal temperatures. Using the inlet coolant temperature instead of the average coolant temperature will result in fictitious magnitudes of $\overline{\varphi}$, $\overline{Y}$, and $(w/\mu)_c$ although the data should still correlate. The average coolant temperature $\overline{T}_c$ can be expressed as a function of the inlet coolant temperature $T_{c,i}$ as given in the following equation:

$$\overline{T}_c = \frac{\eta_t}{2}(\overline{T}_w - T_{c,i}) + T_{c,i} \tag{5}$$

where $\overline{T}_c$ is assumed to be $\frac{1}{2}(T_{c,i} + T_{c,out})$ and where η_t is the airfoil thermal effectiveness and is defined by

$$\eta_t = \frac{T_{c,out} - T_{c,i}}{\overline{T}_w - T_{c,i}} \tag{6}$$

If the relation for T_c is now substituted into equation (2), the following equation results:

$$\frac{\overline{T}_w - T_{c,i}}{\overline{T}_g - \overline{T}_w} \frac{(Pr^{1/3} k)_c}{(Pr^{1/3} k)_g} = K \frac{\left(\frac{w}{\mu}\right)_g^n}{\left(\frac{w}{\mu}\right)_c^m \left[1 - \frac{\eta_t}{2}\right]} \tag{7}$$

The thermal effectiveness η_t can be expressed as a function of only $(w/\mu)_c$. So, although the right hand side of equation is only a function of $(w/\mu)_c$ for a given $(w/\mu)_g$, the data should not be expected to correlate as well as it would if the proper coolant temperature had been used. The original equation is also presented here for the convenience of comparison:

$$\frac{\overline{T}_w - \overline{T}_c}{\overline{T}_g - \overline{T}_w} \frac{(Pr^{1/3} k)_c}{(Pr^{1/3} k)_g} = K \frac{\left(\frac{w}{\mu}\right)_g^n}{\left(\frac{w}{\mu}\right)_c^m} \tag{8}$$

The relative gas temperature $T''_{t,i,r}$ was used in place of the effective gas temperature $T_{g,e}$ in equation (3). This total relative temperature was obtained by correcting the measured average midspan stator-inlet gas temperature $T'_{t,i,s}$ for cooling-air dilution effects and turbine rotational effects. The values of $T''_{t,i,r}$ found by this procedure were used to determine φ values for both local and average conditions. The determination of the gas and coolant properties for use in equations (1) and (2) were also based on the temperatures $T'_{t,i,s}$ and $T_{c,b,i}$ and obtained from reference 8.

It was originally intended that the coolant flow rate to the test blade proper be determined by using the venturi-measured flow rate upstream of the stationary-to-rotating transition point in the blade cooling-air system. The measured flow rate would be corrected to account for leakage into, or out of, the blade cooling-air system that would result from any pressure unbalance across the labyrinth seal and for leakage out through the blade base serrations. During testing, however, it was found that this intended method for determining actual test-blade coolant flow rates was not satisfactory. Difficulties in establishing a near-zero pressure balance across the labyrinth seal knife-edges and uncertainties in pressure measurements resulted in unreliable corrected blade coolant flow rates under rotating conditions. Consequently, it was necessary to deter-

mine the test-blade coolant flow rate analytically. The method used for determining the flow rate is described in appendix B. The correlations of the local and average blade metal temperature data were based on a calculated coolant flow to a blade. The gas flow rate at the inlet to the turbine rotor was considered to be the measured flow through the compressor plus the fuel flow rate and the turbine vane coolant dilution. This total gas flow was then prorated (divided by the number of blades in rotor assembly) to obtain the gas flow rate per blade. The value of the blade coolant flow ratio w_c/w_g was then determined.

In order to make use of the Y correlation equation (eq. (1)), it was necessary to determine the values of the exponents m and n for the quantities $(w/\mu)_c$ and $(w/\mu)_g$. The technique used for determining these values is described fully in reference 3, so, it will be only briefly described herein. A plot of Y against $(w/\mu)_c$ was made for all the data on log-log scale to determine the exponent m. Since the value of $(w/\mu)_g$ is essentially constant for a given series of test points (essentially constant stator-inlet temperature) the plotted data results in a series of curves (nearly parallel straight lines). A least squares curve fit method was used to establish the curves through the plotted data. The resulting slopes of the individual curves were averaged to obtain the value of the exponent m. The above correlation does depend on a knowledge of the local coolant flow. Although a spanwise variation in local flow through these channels will occur because of the spanwise variation in trailing-edge gas pressure and cooling-air pressure, the local flow through the midspan passages (where the heat-transfer analysis is conducted) should approximate an average flow and should approach a constant fraction of the total coolant flow per blade. The value of the exponent n was then obtained from plotting the product $Y(w/\mu)_c^m$ against $(w/\mu)_g$ on a log-log scale. The slope of the resulting curve (a straight line) represents the exponent n. Once again, a least squares fit method was used to establish the curve through the plotted data. A least-squares fit technique was used throughout the correlations whenever a slope or equation of a curve was required.

With the values of the exponents m and n known, the data were plotted on the basis of Y against $(w/\mu)_g^n/(w/\mu)_c^m$. The slope of the curve through the plotted points corresponds to an experimentally determined value of the constant K_1 in equation (1).

When local conditions are considered, exponents m and n are found for each local position in a manner similar to that just described, except that the local values of Y are now used as the ordinates. It should be noted that the values of m and n determined for each local temperature are likely to be different for each local temperature location and differ from those obtained when average temperatures are used.

RESULTS AND DISCUSSION

Each of the five research blades were flow checked before and after heat-transfer testing to insure that the cooling configurations had remained structurally intact. After this testing had been completed, three of the five blades were cut into three spanwise sections, and the other two blades were cut into two chordwise sections so that visual inspection of the blade interior configuration could be made.

This inspection revealed that on two of the blades the two cover plates on the chordwise fins had not been properly joined near the trailing edge during fabrication. As a result, the cooling air entering the internal cavity could be directly expelled through the split trailing edge without performing its intended purpose of cooling the leading edge and midchord regions of the blade.

Since the flow checks indicated that each of the five blades had received approximately equal cooling air flows throughout the heat transfer testing, the temperature data from the remaining three blades was still useful. However, one of these three remaining blades had thermocouples at only the hub section. Therefore, the midspan correlations presented herein contain data from only two of the five blades.

These research blades were tested 355 times of which the first 268 runs are not reported herein. Halfway through these first runs thermocouples at positions 17 and 18 failed. An attempt was made to salvage data from these positions during the first 100 runs since so much other data had to be discarded because of the previously mentioned structural problem. The quantities $1 - \varphi_{17}/\varphi_{17}$ and $1 - \varphi_{18}/\varphi_{18}$ correlated quite well with $1 - \varphi_{20}/\varphi_{20}$ as they should since these three thermocouples are all on the same blade. These two correlations, established using the early data, were then used to calculate temperatures at positions 17 and 18 for the later data which are presented herein. These calculated temperatures were then used to establish an average blade temperature whenever one was needed. This same procedure could not be used with the trailing edge thermocouples, positions 13 and 19, since these failed at the very start of the test program.

The data, information, and techniques used in an attempt to correlate data over the range of conditions listed in table II are discussed in this section. Successful correlation of data will provide empirical methods of calculating blade airfoil temperatures at conditions other than those investigated and will provide a basis for comparing blades of different cooling geometries designed for conditions similar to those presented in this report.

Chordwise Blade Temperature Distribution

Typical curves of blade wall temperature distributions for the 3.81-centimeter (1.5-in.) span position are shown in figure 9 for a nominal inlet gas temperature to the stator $T'_{t,i,s}$ of 1656 K (2521° F), a nominal blade inlet coolant temperature $T_{c,b,i}$ of 361 K (190° F), and varying coolant flow ratios w_c/w_g from 0.029 to 0.111. At this stator-inlet temperature, the nominal relative gas temperature $T''_{t,i,r}$ was 1489 K (2221° F). As expected, the blade wall temperature T_w increases with an accompanying decrease in coolant flow ratio w_c/w_g, and the temperature distributions exhibit similar general characteristics. It is readily apparent that extreme temperature gradients have resulted and that there is also some overcooling of the midchord suction surface with respect to that of the midchord pressure surface. This can be explained by the fact that 60 percent of the cooling airflow is directed to the suction surface of the blade. The curves reveal a maximum temperature difference of 460 K (828° F) (from the leading edge to the midchord suction surface), which is considerably higher than that which is desirable for extended blade life. A temperature gradient of about 167 K (300° F) is generally acceptable.

Figure 10 shows typical blade wall temperature distributions for a nominal inlet gas temperature to the stator of 1382 K (2028° F), a nominal coolant flow ratio of 0.03, and inlet coolant temperatures of approximately 379 K (223° F), 485 K (413° F), and 699 K (798° F). For this stator inlet temperature, the relative gas temperature was approximately 1262 K (1812° F). As in figure 9, the curves of figure 10 once again exhibit similar trends. For this lower stator-inlet temperature, the maximum chordwise wall temperature difference is approximately 325 K (585° F). As the coolant temperature increases, the difference between the maximum and minimum temperatures decreases until, in the limit, it approaches zero when the coolant temperature approaches the gas temperature.

Spanwise Blade Temperature Distribution

Only a limited amount of spanwise temperature data are available because of the inability to instrument the thin wall near the blade tip. The most severe temperature gradient occurred at the leading edge between the 1.27- and the 3.81-centimeter (0.5- and 1.5-in.) span positions, where a temperature difference of approximately 200 K (360° F) existed. The location of the thermocouples at various spanwise and chordwise positions and the associated temperatures can be obtained from tables I and II.

Correlation of Average Blade Temperatures at 3.81-Centimeter (1.5-in.) Span Position

The successful correlation of the average blade wall temperatures near the blade midspan can provide an indication of the overall effectiveness of the blade cooling geometry. However, since averaging may mask some extreme temperature gradients, a correlation of local blade wall temperatures is also of importance and will be discussed in a later section.

For the purpose of the following correlations, the average blade temperature $\overline{T}_w$ is considered to be the integrated average of the local thermocouples located on the blades at the 3.81-centimeter (1.5-in.) span position. The correlation parameter $\overline{\varphi}$ was based on the integrated average blade wall temperature $\overline{T}_w$, the relative gas temperature $T''_{t,i,r}$, and the cooling air temperature at the inlet to the blade base $T_{c,b,i}$. Those gas and coolant properties required in the correlation of the data were based on the respective $T'_{t,i,s}$ and $T_{c,b,i}$. The following correlations for average blade temperatures includes the midspan data from thermocouple positions 12, 14, 15, 20, and 21 from table II plus correlated values of temperature for thermocouple position 17 and 18. A particular symbol is defined for each series of test points listed and is common for all the figures presented.

$\overline{Y}$ correlation. - In order to make use of the Y correlation equation, (eq. (1)), it was necessary to determine the values of the exponents m and n for the quantities $(w/\mu)_c$ and $(w/\mu)_g$. As described previously, a least squares curve fit method was used to establish the curves through each series of plotted data. The resulting slopes of the individual curves were averaged to obtain the value of the exponent m, which for these data was 0.64. The value of the exponent n was then obtained from plotting the product $\overline{Y}(w/\mu)_c^{0.64}$ against $(w/\mu)_g$ on a log-log-scale. The slope of the resulting curve (a straight line) represents the exponent n, which for these data has a value of 0.59.

With the values of the exponents m and n known, the data were plotted on the basis of $\overline{Y}$ against $(w/\mu)_g^{0.59}/(w/\mu)_c^{0.64}$ and are presented in figure 11. The slope of the curve through the plotted points corresponds to an experimentally determined value of the constant K_1 in equation (1). The value of this slope for the data presented in the figure is 0.095 $(cm^{0.05})$. For this plot, equation (1) becomes $\overline{Y} = 0.095\ (w/\mu)_g^{0.59}/(w/\mu)_c^{0.64}$ where (w/μ) has units of centimeters.

As can be seen from the figure and table II, the data having the higher coolant inlet temperatures (test series 6 and 7 of table II) do not correlate in the same way as do the data having the lower coolant inlet temperatures (test series 1 to 5). Therefore, these

data were not used in establishing the correlation equation. Also, the lines showing the data scatter refer to only the data having the lower coolant inlet temperature.

The scatter of data lies within a band of about ±10 percent deviation from the least squares determined curve fit and is represented in the figure by the dashed lines. The scatter of data resulting for this correlation may be due in part to the fact that a blade inlet coolant temperature was used, rather than a more representative coolant temperature within the blade airfoil, for obtaining property values and in the determination of $\overline{Y}$. As coolant flow to the blade is decreased, the temperature rise of the coolant from the blade inlet to the location within the airfoil being evaluated increases, and the inlet coolant temperature becomes less representative of the average coolant temperature within the airfoil.

Correlation of $(1 - \overline{\varphi})/\overline{\varphi}$. - Elimination of gas and coolant property values from equation (1) results in a simplified correlation whereby $(1 - \overline{\varphi})/\overline{\varphi}$ can then be plotted against $(w_g)^m/(w_c)^n$. Of course, new values of the exponents m and n must be determined in the same manner as that for the $\overline{Y}$ correlation. The values determined for the exponents m and n were 0.51 and 0.64, respectively. No figures are presented for this correlation method since the scatter of data points was similar to that for the $\overline{Y}$ correlation.

Correlation of $\overline{\varphi}$. - A further simplification of equation (1) permits correlating the data by plotting $\overline{\varphi}$, the temperature difference ratio, against w_c/w_g, the ratio of coolant-to-gas flow rates. The data based on this correlation is presented in figure 12. Despite its simplification, this correlation results in the least scatter of data. The correlation of data is good, and, except for the data having the higher coolant inlet temperatures which were not used in establishing the correlation, the maximum deviation from the least squares fit is about ±3 percent. The resulting equation of the least squares curve fit for this correlation is given on the figure; it is

$$\overline{\varphi} = \frac{1}{1 + 0.10\left(\frac{w_c}{w_g}\right)^{-0.59}} \tag{9}$$

Correlation of Local Temperatures at 3.81 Centimeters (1.5 in.) Span Position

Methods similar to those used for correlating the average temperature data are also used for correlating the local temperature data at the 3.81-centimeter (1.5-in.) span position. The correlations are based on local measured blade wall temperatures, the relative gas temperature at the 3.81-centimeter (1.5-in.) span position, the coolant temperature at the inlet to the blade, and the gas and coolant properties associated with

the latter two temperatures. In addition, the correlations are based on the total coolant flow rate to the blade airfoil rather than the actual local coolant flow distribution within the airfoil.

Correlation of Y_x. - Figure 13 presents the Y_x correlation for local blade temperatures at four of the seven thermocouple locations, 12, 14, 15 and 20, around the blade periphery at the 3.81-centimeter (1.5-in.) span position. Data from thermocouple 21 is also presented which is a duplication of position 15 but on an adjacent blade. As can be seen from table II, the thermocouples at the other three locations were lost relatively early in the test program. The exponents m and n for the two terms $(w/\mu)_c$ and $(w/\mu)_g$ in the abscissa were determined for each thermocouple location in the same manner as that for the $\overline{Y}$ correlation and their values are shown in the individual plots.

As in the case of the $\overline{Y}$ correlation, the data scatter is attributed in part to the use of the blade inlet coolant temperature $T_{c,b,i}$ rather than the local coolant temperature. In addition, some data scatter may be attributed to the fact that the total coolant flow is used in the correlation of data rather than the more representative local coolant flow rate. This would be particularly true regarding the midchord pressure surface and midchord suction surface regions because the total flow is divided between these regions. Each individual plot has bands of the data scatter represented by the dashed lines. The best of the local correlations was for thermocouple 15 (fig. 13(e)), which resulted in data scatter bands of +5 and -11 percent deviation from the least squares curve through the data points. The worst of the local correlations was for thermocouple 12 (fig. 13(a)), which had data scatter bands of +8 and -14 percent. As before, the data scatter bands refer only to the data of the first five series in table II.

The values of n appearing in figure 13 represent the experimentally obtained values of the exponent of the Reynolds number for the gas-to-wall heat-transfer coefficient. The value of 0.69 (from fig. 13(a)) represents the exponent near the trailing edge of the suction surface. The values of 0.58 and 0.56 (from figs. 13(c) and (d) represent the exponents for the midchord and the trailing edge of the pressure surface, respectively. The values of 0.59 and 0.65 (from figs. 13(b) and (e)) both represent the exponent for the point 80° from the stagnation point on the pressure surface. These five values around the blade periphery are less than 0.8, indicating that the flow is transitional. In general, flow over the suction surface is closer to being turbulent than that for the pressure surface (0.69 against 0.58 and 0.56, respectively). The data for the leading edge (0.59 and 0.65) indicate a deviation from the commonly accepted value of 0.5 for laminar flow.

Correlation of φ_x. - Figure 14 shows the local temperature difference ratio φ_x as a function of the ratio of total blade coolant to gas flow for the same thermocouples

considered in figure 13. The correlation equations for the least squares curves through the data are given for each thermocouple in figure 14 and also in table III. Deviations of data from the respective correlations were calculated and found to be less than the deviations of data from the Y_x correlation for each thermocouple considered. The maximum deviation of plotted data from any respective curve was found to be about ±7 percent (see thermocouple 12, fig. 14(a)).

Although it is not presented in figure 14 thermocouple 18 exhibits a φ_x value of 0.69 for a coolant flow ratio of 0.03. This relatively high value of φ_x can be justified based on predicted values of the local gas-to-wall and wall-to-coolant heat-transfer coefficients. If the wall-to-coolant heat-transfer coefficient is adjusted to include entrance effects and fin effectiveness, the resulting analytical value of φ_x compares very favorably with the experimental results.

Impingement cooling of the leading edge resulted in relatively low values of φ_x. At the location of thermocouple 17 the experimental value of φ_x was 0.33 for a coolant-to-gas flow ratio of 0.03. However, if an optimum impingement geometry had been incorporated in the cooling design for the leading edge region, the local value of φ_x would have been approximately 0.42.

Comparison of Measured Temperature with Temperature Obtained from Correlations

Average temperature. - The scatter bands for the data in figures 11 and 12 ($\overline{Y}$ against $(w/\mu)_g^n/(w/\mu)_c^m$ and $\overline{\varphi}$ against w_c/w_g, respectively) are based on temperature difference ratios. As such it is often difficult to readily determine what the scatter is in terms of temperature. Figures 15 and 16 show the scatter between measured temperatures and those determined from the correlation equations in order to illustrate the scatter based on this method.

Because the data with the higher coolant inlet temperatures were not used when the correlation was established, it is significant that these data agree as well as they do with the temperatures determined using the correlation. Respective error bands of ±3 percent and ±2.5 percent are shown on these figures for the $\overline{Y}$ and $\overline{\varphi}$ correlations, respectively. Inspection of the figures shows the $\overline{\varphi}$ correlation to be superior to the $\overline{Y}$ correlation. This fact, plus the ease in application of the $\overline{\varphi}$ correlation, indicates that the $\overline{\varphi}$ correlation should be used for estimating average blade temperatures (at least for the blade considered herein).

Local temperature. - The scatter bands for the data in figures 13 and 14 (Y_x against $(w/\mu)_g^n/(w/\mu)_c^m$ and φ_x against w_c/w_g, respectively) are also based on tem-

perature difference ratios. The scatter between the measured temperatures and the experimentally determined φ_x correlation equations are within ±4 percent. The corresponding scatter of the data from the Y_x correlation equations as a group are greater than those from the φ_x correlation equations.

Blade Operating Potential

Because the original rotor blade design exhibited an undesirably high leading edge temperature and a severe temperature gradient as can be seen in figures 9 and 10, a redesign of the blade was undertaken. The optimum spacing between the impingement holes and the inner surface of the leading edge of the blade to decrease the maximum temperature was obtained from figure 9 of reference 9. The fin geometry along the blade suction and pressure surfaces was changed to reduce the temperature gradient while decreasing the average temperature. The differences between the original and revised blade designs are that (1) the spacing between the impingement holes and the inner blade leading edge surface was reduced from 8 to 2 equivalent slot widths, (2) the fin thickness along the blade suction surface was increased from 0.0508 centimeter (0.02 in.) to 0.084 centimeter (0.033 in.); and (3) the fin thickness along the pressure surface was decreased from 0.127 centimeter (0.05 in.) to 0.0508 centimeter (0.02 in.). These changes in fin thickness resulted in a reduction of the number of chordwise passages along the suction surface from 80 to 64 and an increase along the pressure surface from 50 to 80.

A comparison of the experimental midspan chordwise blade temperature distribution for the original blade design with the calculated temperature distribution for the revised blade design is shown in figure 17 for a coolant to gas flow ratio of 0.03, a coolant inlet temperature of 922 K (1200° F), and a relative gas temperature of 1496 K (2232° F). This chordwise temperature distribution for the revised design was calculated from the following equation (which corrects correlated wall temperatures from the original design for a revised coolant to wall heat-transfer coefficient) using calculated inside heat-transfer coefficients and the constants from table III.

$$h_c\left[\frac{(1 - \varphi_x)}{\varphi_x}\right]_{original} = h_c\left[\frac{(1 - \varphi_x)}{\varphi_x}\right]_{revised}$$

The chordwise temperature distribution for the original design was calculated using the constants in table III.

As can be seen from the temperature distribution of figure 17, the maximum temperature decreased from 1309 K (1896° F) to 1256 K (1800° F), the average temperature

decreased from 1175 K (1655° F) 1166 K (1639° F) and the difference between the maximum and minimum temperatures decreased from 212 K (382° F) 120 K (216° F). The reason that temperature gradients are lower in figure 17 than in figure 9 for similar coolant flows and gas temperatures results from the very low cooling-air temperature used in obtaining the experimental data in figure 9. The intent of presenting the chordwise temperature distribution for the blade with the revised geometry is merely to demonstrate that a blade design having an impingement cooled leading edge and chordwise coolant passage is feasible.

The hot spot on the original design was found to be the blade leading edge. Using the local correlation for this position, and coolant and metal temperatures of 922 K (1200° F) and 1256 K (1800° F), respectively, the potential stator-inlet temperature was calculated for a range of values of w_c/w_g. The relation between stator-inlet temperature and relative gas temperature is a function of the stator-exit Mach number and the relative rotor-inlet Mach number. For an experimentally determined midspan stator-exit Mach number of 0.885 and a design relative rotor-inlet Mach number of 0.475, the ratio of stator-inlet total temperature to relative rotor-inlet temperature is 10/9. This value is substantiated by the direct calculation of the relative gas temperature. The decreases in the effective gas temperature due to both dilution from the stator and rotation of the turbine wheel are calculated separately and then subtracted from the stator-inlet temperature to yield the relative gas temperature. Results of such calculations are presented in the discussion of figures 9 and 10. For the conditions listed in these figures the ratios of the stator inlet total temperature to relative gas temperature are 1.124 and 1.104, respectively, or approximately 10/9. This value of 10/9 was used to calculate potential stator-inlet temperatures from relative gas temperatures.

The potential stator-inlet gas temperature for both the original and new blade designs are plotted in figure 18. The figure shows, for example, that for $w_c/w_g = 0.03$ the redesigned blade can operate at a stator-inlet temperature of 1662 K (2532° F) whereas the original designed blade can operate at 1574 K (2374° F). In addition, the blade with the original design would have large temperature gradients that would limit its life.

SUMMARY OF RESULTS

The results of the experimental investigation reported herein are summarized as follows:

1. Experimental heat-transfer data for an air-cooled turbine rotor blade design incorporating an impingement-cooled leading edge, chordwise-coolant passages in the midchord region, and a slotted trailing edge for expelling coolant were successfully

correlated at stator-inlet gas temperatures up to 1657 K (2523° F). Both average and local blade temperatures were included.

2. The simplest of the correlations, the temperature difference ratio φ as a function of the coolant flow ratio w_c/w_g resulted in the best agreement of the data. It is therefore the recommended correlation for obtaining additional blade temperature information for similar test conditions.

3. The maximum deviation of measured local and average temperatures at the 3.81-centimeter (1.5-in.) span position from those calculated using the φ_x and $\overline{\varphi}$ correlations, respectively, was ±3 percent. The value $\overline{\varphi}$ for the blade tested in the engine was 0.56 for a coolant-to-gas flow ratio of 0.03.

4. Because the original blade design exhibited large temperature gradients and a hot leading edge, a design study was made of a revised internal fin arrangement and leading-edge impingement cooling configuration. The following table presents the results of that design study:

	Original vane	Revised vane
Turbine stator inlet temperature, K (°F)	1662 (2532)	1662 (2532)
Relative gas temperature, K (°F)	1496 (2232)	1496 (2232)
Coolant inlet temperature, K (°F)	922 (1200)	922 (1200)
Coolant to gas flow ratio	0.03	0.03
Maximum wall temperature, K (°F)	1309 (1896)	1256 (1800)
Average wall temperature, K (°F)	1175 (1655)	1166 (1639)
Maximum temperature difference, K (°F)	212 (382)	120 (216)

5. For a coolant-inlet temperature of 922 K (1200° F) and a coolant-to-gas-flow ratio of 0.03, the revised blade design was shown to have potential application for a stator inlet temperature of 1662 K (2532° F), whereas a blade with the original design has only a corresponding temperature of 1574 K (2374° F).

Lewis Research Center,
National Aeronautics and Space Administration,
Cleveland, Ohio, December 7, 1971,
764-74.

APPENDIX A

SYMBOLS

A	flow area
C	dimensional constant
c_p	specific heat
G	mass flow rate per unit area
g_c	conversion factor in Newton's law of motion
h	heat-transfer coefficient
K	dimensional constant
k	thermal conductivity
L	surface distance from leading edge to trailing edge
LE	leading edge
L_p	surface distance from leading edge along pressure surface
L_s	surface distance from leading edge along suction surface
m	exponent
n	exponent
p	pressure (static, if not accompained with superscript ')
Pr	Prandtl number
Q	heat flux
r	radius
T	temperature
TE	trailing edge
w	mass flow rate
x	distance along blade surface from extreme leading edge (stagnation point)
Y	data correlation factor (see eqs. (1) and (2))
η_t	airfoil thermal effectiveness
μ	viscosity
ρ	density

φ	temperature difference ratio (see eq. (3))
ω	angular velocity

Subscripts:

b	blade
c	coolant
corr	correlation
e	effective
f	friction
g	gas
i	inlet
in	inlet to coolant flow station
m	momentum
meas	measured
out	outlet from coolant flow station
r	rotor
S	surface
s	stator
SL	serration leakage
t	turbine
w	wall (blade, unless otherwise specified)
x	local
ω	rotation
1, 2	denotes either specific constant or cooling air flow system station
3, 4, 5, 6	cooling air flow system stations

Superscripts:

'	total condition
''	total relative condition
—	average

APPENDIX B

DETERMINATION OF TEST BLADE COOLANT FLOW

A calculation method was used to determine the test blade coolant flow. The method used a set of four static calibration curves in conjunction with experimental engine data. The calibration curves related coolant flow to friction pressure drop between adjacent stations of the test blade coolant flow system which is shown in figure 4. The experimental engine data were used to define the state conditions of the cooling air in various sections of the test-blade cooling-air systems. The locations of these thermocouples and pressure taps are also shown in figure 4. Figure 19 is a flow chart of the method used in this calculation.

The method presented in figure 19 essentially consists of superimposing momentum pressure loss and rotational pressure rise on the calibrated friction pressure drop between two stations. This would either determine, by iteration, a pressure if the coolant flow is assumed, as in the case of progressing from station 1 to 2 to 3, or a coolant flow if the pressures are assumed, as is the case between stations 3 and 4. When the coolant flow used in the calculations between stations 2 and 3 converges to the coolant flow calculated between stations 3 and 4, an answer is assumed. A calibration is used to calculate the blade serration leakage knowing the pressures at stations 2 and 5. Calibrations for the friction static-pressure drop are of the form

$$\bar{\rho}\ \Delta p_f = f(w) \tag{B1}$$

The momentum pressure drop between stations,

$$\Delta p_m = \frac{\bar{G}}{g_c}\left(\frac{G_{out}}{\rho_{out}} - \frac{G_{in}}{\rho_{in}}\right) \tag{B2}$$

and the rotational pressure rise between stations,

$$\Delta p_\omega = \frac{\bar{\rho}\omega^2\left(r_{out}^2 - r_{in}^2\right)}{2g_c} \tag{B3}$$

are presented in reference 5. The subscripts in and out refer to the inlet and outlet of a particular section under consideration. Because few cooling air temperatures were

measured, various assumptions about coolant temperatures were made in these calculations.

REFERENCES

1. Stepka, Francis S.; and Richards, Hadley T.: Experimental Investigation of Metal Temperatures of Air-Cooled Airfoil Leading Edges at Subsonic Flow and Gas Temperatures up to 2780° F. NASA TN D-127, 1959.

2. Livingood, John N. B.; and Brown, W. Bryon: Analysis of Spanwise Temperature Distribution in Three Types of Air-Cooled Turbine Blades. NACA Rep. 994, 1950.

3. Gladden, Herbert J.; Gauntner, Daniel J.; and Livingood, John N. B.: Analysis of Heat-Transfer Tests of an Impingement, Convection, Film Cooled Vane in a Cascade. NASA TM X-2376, 1971.

4. Calvert, Howard F.; Cochran, Reeves P.; Dengler, Robert P.; Hickel, Robert O.; and Norris, James W.: Turbine Cooling Research Facility. NASA TM X-1927, 1970.

5. Yeh, Frederick, C.; Poferl, David J.; Cochran, Reeves P.; and Richards, Hadley T.: Cooling Airflow Study Through a Stationary Turbine Disk and Blade. NASA TM X-2171, 1971.

6. Kaufman, A.; Berry, T. F.; and Meiners, K. E.: Joining Techniques for Fabrication of Composite Air-Cooled Turbine Blades and Vanes. Paper 71-GT-32, ASME, Mar. 1971.

7. Crowl, Robert J.; and Gladden, Herbert J.: Methods and Procedures for Evaluating, Forming, and Installing Small-Diameter Sheathed Thermocouple Wire and Sheathed Thermocouples. NASA TM X-2377, 1971.

8. Poferl, David J.; Svehla, Roger A.; and Lewandowski, Kenneth: Thermodynamic and Transport Properties of Air and the Combustion Products of Natural Gas and of ASTM-A-1 Fuel with Air. NASA TN D-5452, 1969.

9. Metzger, D. E.; Yamashita, T.; and Jenkins, C. W.: Impingement Cooling of Concave Surfaces with Lines of Circular Air Jets. Paper 68-WA/GT-1, ASME, Dec. 1968.

TABLE I. - BLADE THERMOCOUPLE LOCATIONS

Suction surface						Pressure surface					
Thermocouple number	Leading- to trailing edge surface distance, L_s		Surface distance, x		Dimensionless surface distance, x/L_s	Thermocouple number	Leading- to trailing edge surface distance, L_p		Surface distance, x		Dimensionless surface distance, x/L_p
	cm	in.	cm	in.			cm	in.	cm	in.	
3.81 cm (1.5 in.) above blade platform											
5 and 7	4.991	1.965	0.048	0.019	0.010	9, 15, and 21	4.511	1.776	0.381	0.150	0.084
6 and 12	↓	↓	3.581	1.410	.718	8 and 14	↓	↓	1.499	.590	.334
18 and 23	↓	↓	1.976	.778	.396	7 and 20	↓	↓	2.794	1.100	.619
13 and 19	↓	↓	4.293	1.690	.860		↓	↓			
1.27 cm (0.5 in.) above blade platform											
1	5.265	2.073	0.381	0.150	0.072	3	4.707	1.853	3.025	1.191	0.643
2	5.265	2.073	4.115	1.620	.781	4	4.707	1.853	.381	.150	.081
5.08 cm (2.0 in.) above blade platform											
22	4.859	1.913	0.381	0.150	0.078	25	4.422	1.741	2.794	1.100	0.632
24	4.859	1.913	3.581	1.410	.737	26	4.422	1.741	.381	.150	.086

TABLE II. - SUMMARY OF ENGINE OPERATING CONDITIONS AND BLADE TEMPERATURES

Series	Symbol	Run	Engine speed, rpm	Turbine stator inlet temperature, K	Relative turbine rotor inlet temperature, K	Blade coolant-to-gas flow ratio	Blade cooling air inlet temperature, K	Blade metal temperature, K										Gas flow per blade channel, kg/sec
								Thermocouple numbers[a, b]										
							10	16	1	3	4	11	12	14	15	20	21	
1	○	269	8360	1657	1489	0.1112	341	330	804	684	823	667	496	651	792	706	791	0.3523
		270	8375	1655	1488	.0904	344	330	831	717	849	610	521	683	825	743	827	.3530
		271	8576	1656	1491	.0646	361	367	879	776	898	689	576	744	878	807	883	.3625
		272	8652	1653	1484	.0356	394	407	947	875	962	758	694	864	971	921	970	.3671
		273	8673	1657	1489	.0291	409	424	968	908	983	782	745	903	1002	965	1007	.3670
2	□	288	7909	1493	1363	0.1254	334	334	743	627	764	461	458	597	721	643	720	0.3307
		289	7982	1477	1349	.1037	341	342	765	652	787	534	480	621	744	668	743	.3353
		290	8045	1478	1349	.0846	351	353	802	694	823	604	513	663	783	711	783	.3397
		294	8083	1474	1346	.0389	379	371	889	814	904	698	636	794	892	851	898	.3407
		295	8099	1473	1344	.0297	391	378	913	852	927	(c)	691	838	927	898	934	.3421
		296	8129	1467	1337	.0257	401	389	934	882	947	↓	727	867	950	927	956	.3448
		297	8197	1469	1341	.0190	421	431	966	930	979	↓	797	923	998	980	1000	.3485
		298	8198	1476	1347	.0182	422	431	968	931	982	↓	798	924	998	982	1002	.3477
		299	8186	1473	1344	.0189	421	405	964	924	977	↓	787	915	991	973	994	.3479
3	▷	300	7396	1393	1269	0.1332	326	326	694	589	714	(c)	447	562	674	603	672	0.3048
		301	7416	1383	1261	.1111	329	329	712	607	733	↓	465	578	692	621	690	.3080
		302	7471	1380	1259	.0892	337	337	743	641	763	↓	492	611	723	656	723	.3111
		303	7477	1375	1255	.0726	342	342	764	669	784	↓	516	642	752	689	753	.3114
		304	7495	1374	1255	.0531	350	350	796	711	813	↓	554	689	792	737	793	.3118
		305	7579	1382	1262	.0415	359	362	828	753	844	↓	594	733	828	786	833	.3170
		306	7655	1396	1276	.0290	379	378	875	817	888	↓	668	801	884	859	891	.3216
		307	7710	1397	1278	.0187	397	395	914	874	926	↓	741	863	936	921	940	.3239
4	▽	309	8232	1577	1427	0.1230	338	332	778	657	800	(c)	473	622	754	673	754	0.3424
		310	8297	1575	1427	.1002	348	346	808	690	831	↓	501	656	787	708	788	.3462
		311	8375	1579	1433	.0737	361	393	851	741	873	↓	547	708	837	760	836	.3507
		312	8383	1574	1429	.0606	371	378	879	779	899	↓	583	751	872	805	875	.3504
		313	8381	1576	1431	.0603	371	380	880	780	901	↓	584	752	873	806	875	.3510
		314	8408	1544	1402	.0484	382	389	908	819	923	↓	626	797	908	852	912	.3509
		315	8516	1591	1448	.0363	398	414	951	876	968	↓	690	857	960	918	970	.3565
		317	8603	1579	1428	.0236	432	436	1008	959	1022	↓	805	946	1033	1012	1041	.3609
		318	8615	1583	1433	.0174	451	448	1034	1000	1049	↓	864	995	1075	1056	1078	.3611
5	◁	330	7786	1356	1252	0.0736	347	349	721	637	748	(c)	498	618	733	659	728	0.4661
		332	7884	1341	1238	.0467	371	372	787	713	811	↓	569	703	811	748	809	.4673
		333	7901	1352	1250	.0467	371	373	795	720	819	↓	580	709	818	753	815	.4676
		334	7923	1354	1253	.0384	382	383	816	740	839	↓	604	743	845	787	843	.4680
		335	7931	1351	1250	.0299	394	396	839	783	861	↓	646	783	874	829	874	.4683
		336	7957	1354	1251	.0204	416	417	876	836	896	↓	717	842	922	892	922	.4682
		337	8058	1361	1253	.0177	435	438	907	877	924	↓	759	876	948	926	950	.4718
		338	8053	1361	1258	.0175	437	440	904	876	922	↓	762	877	949	926	951	.4690
6	▷	340	7264	1376	1234	0.1078	483	429	768	703	781	(c)	593	694	776	722	773	0.3082
		341	7245	1375	1250	.0906	482	436	792	723	806	↓	609	712	797	743	794	.2955
		342	7329	1372	1247	.0717	488	443	819	750	834	↓	635	738	818	770	818	.3031
		343	7375	1379	1255	.0602	491	448	837	772	851	↓	655	763	841	795	841	.3060
		344	7394	1375	1253	.0477	492	483	853	794	867	↓	678	788	862	821	863	.3069
		345	7398	1376	1254	.0397	491	494	869	815	882	↓	703	812	882	846	883	.3055
		346	7492	1386	1264	.0270	508	495	908	870	919	↓	768	873	934	913	937	.3115
		347	7584	1383	1262	.0221	518	505	933	902	945	↓	802	903	961	945	963	.3161
		348	7489	1382	1262	.0312	485	454	900	856	912	↓	743	853	920	894	921	.3113
		349	7452	1383	1264	.0422	455	432	860	803	873	↓	674	797	873	834	874	.3078
7	▢	350	7676	1383	1254	0.0708	699	598	919	886	926	(c)	799	887	937	904	938	0.3257
		351	7664	1383	1256	.0590	695	593	931	897	940	↓	811	898	947	916	948	.3256
		352	7709	1377	1259	.0399	698	606	958	926	968	↓	846	928	974	949	976	.3263
		353	7631	1374	1257	.0335	699	607	966	939	974	↓	863	945	989	968	991	.3189
		354	7618	1351	1236	.0246	688	631	978	958	987	↓	884	966	1008	993	1010	.3185
		355	7608	1351	1236	.0248	691	644	979	961	989	↓	887	967	1010	994	1012	.3175

[a]Thermocouple numbers and locations are shown in fig. 8.

[b]Thermocouples 2, 5 to 9, 13, 17 to 19, 22, and 23 were inoperative during these tests.

[c]Inoperative from run 295 on.

TABLE III. - VALUES OF CONSTANTS AND EXPONENTS FOR BASIC CORRELATING EQUATION OF LOCAL TEMPERATURE DIFFERENCE RATIO[a]

$$\left[\varphi_x = \frac{1}{1 + E(w_c/w_g)^F}\right]$$

Thermocouple	Constant, E	Exponent, F
17	0.47	-0.42
18	.04	-.70
12	.028	-.80
21	.20	-.53
15	.20	-.52
14	.09	-.64
20	.11	-.66

[a]See fig. 14.

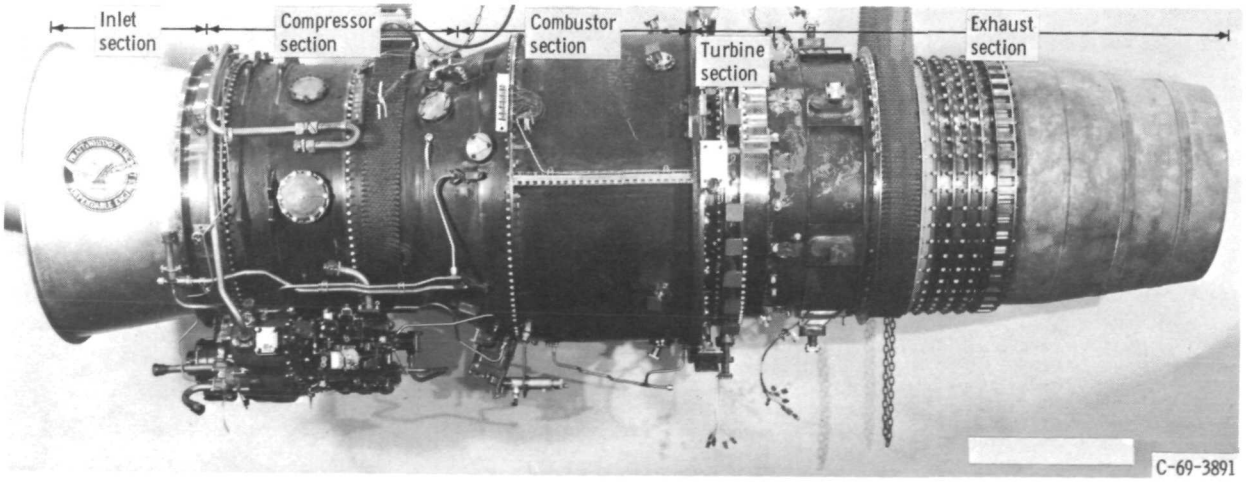

Figure 1. - Turbine cooling research engine.

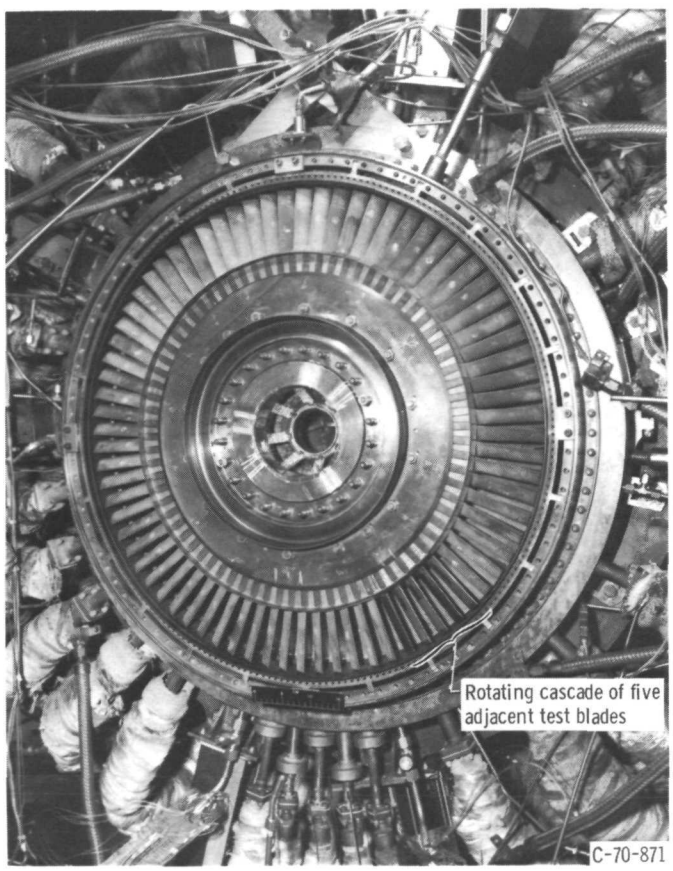

Figure 2. - View of air-cooled turbine rotor in research engine.

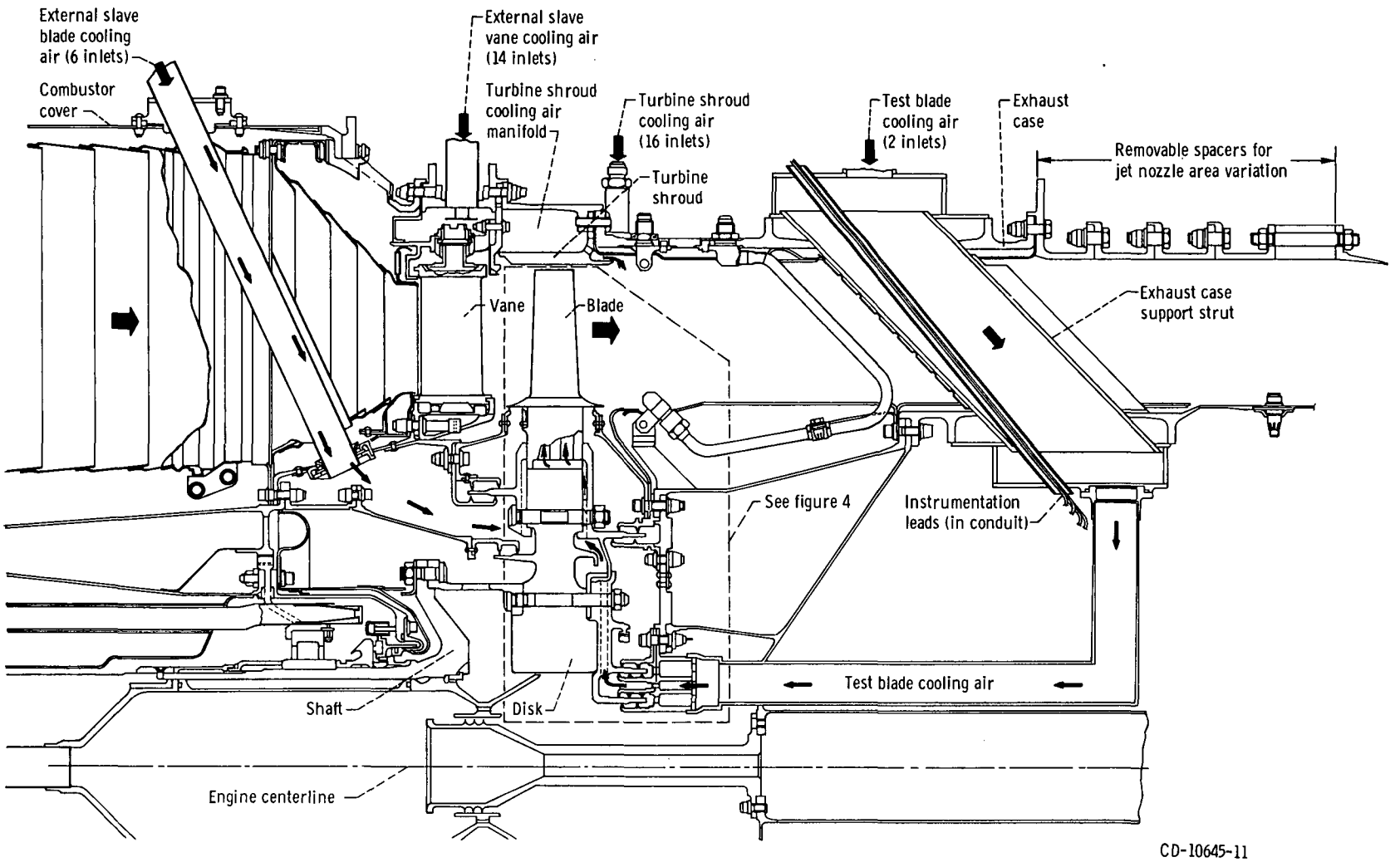

Figure 3. - Hot section of turbine cooling research engine.

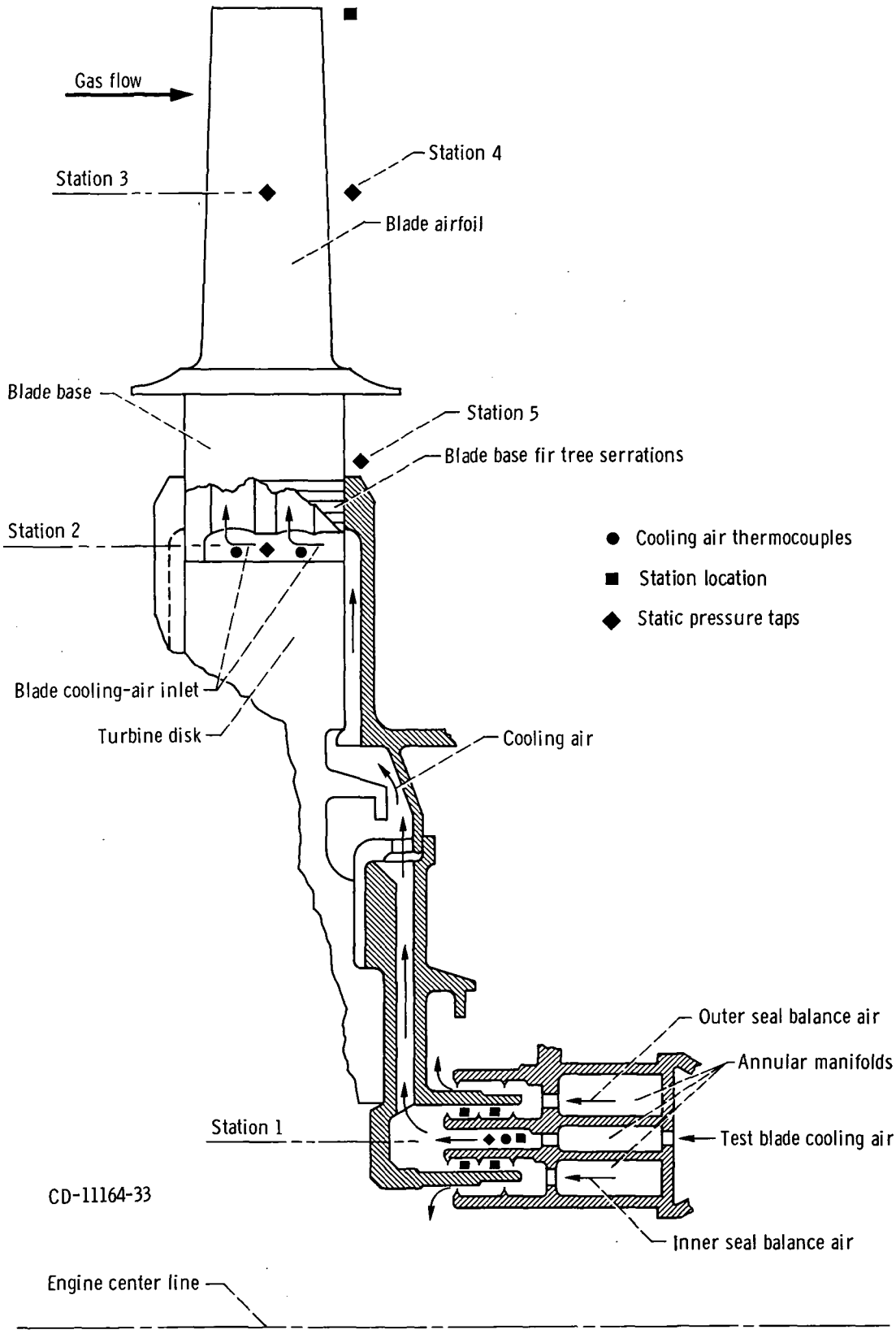

Figure 4. - Balanced pressure cooling-air labyrinth seal system.

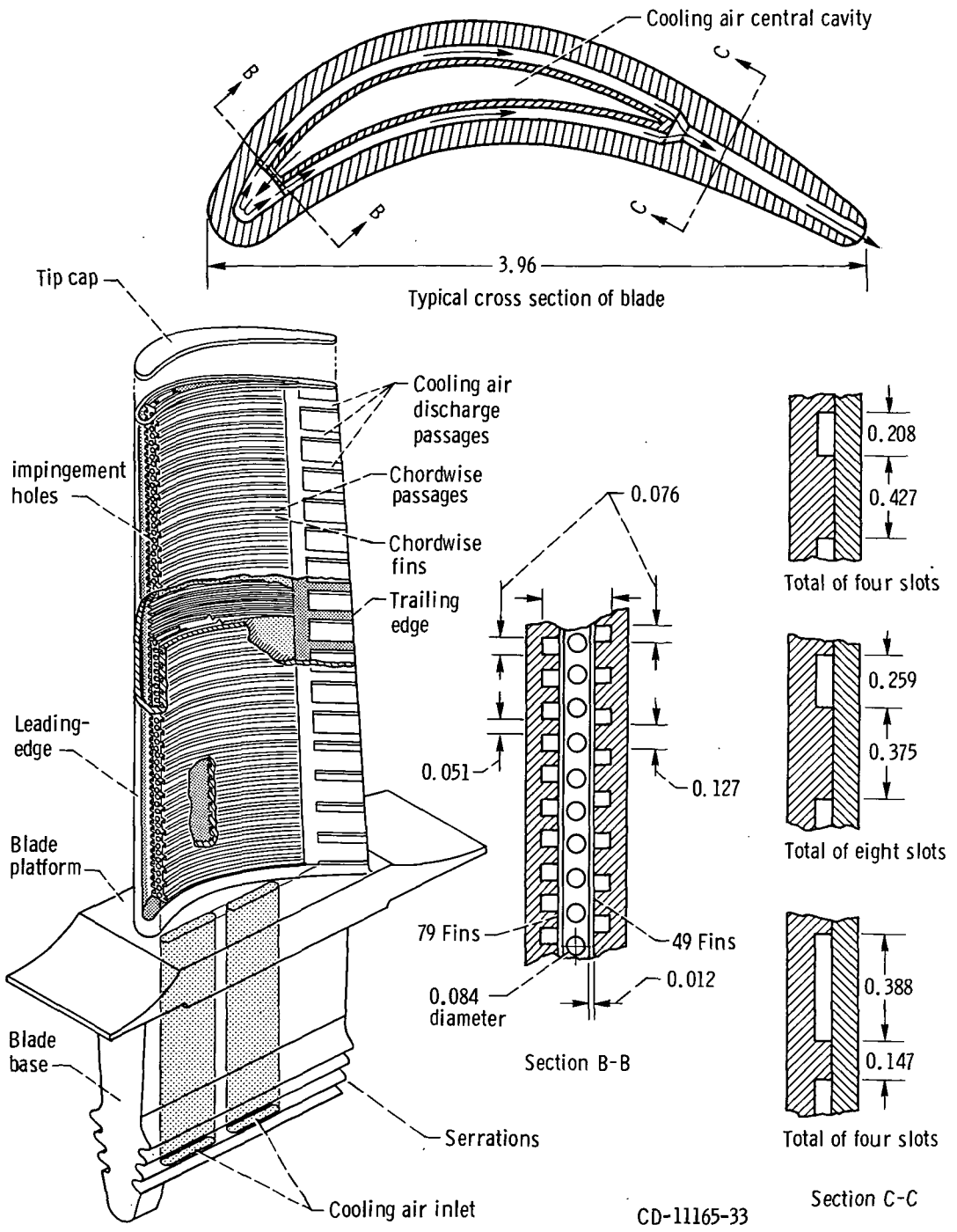

Figure 5. - Cut-away schematic of chordwise-passage air-cooled blade. (All dimensions are in centimeters.)

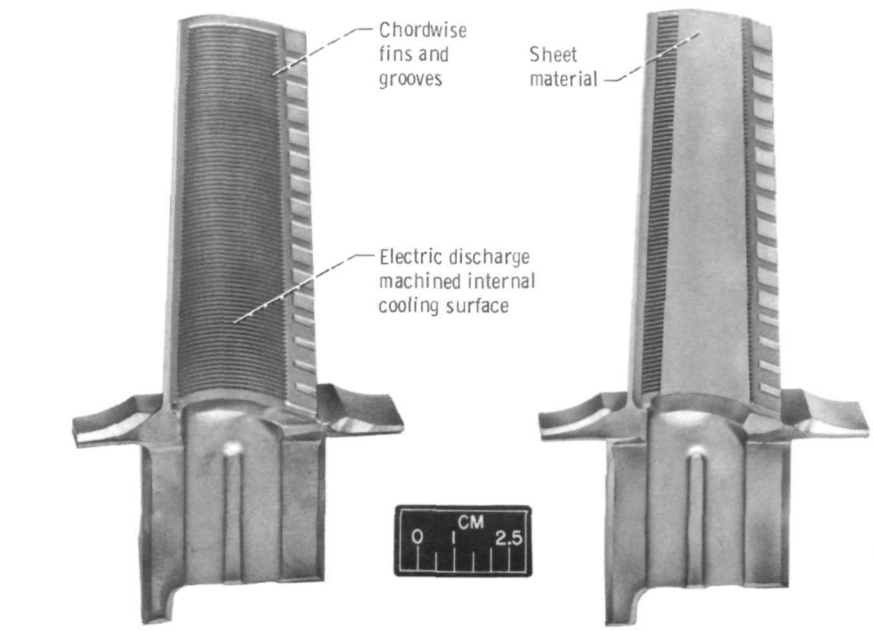

(a) Suction side blade half.

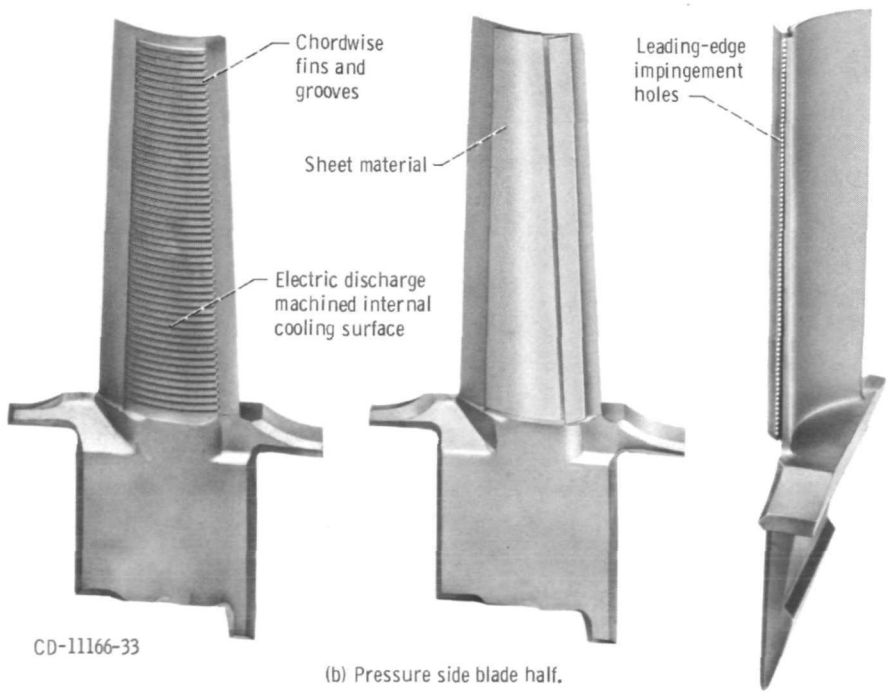

(b) Pressure side blade half.

Figure 6. - Subassembly of chordwise-passage blade halves.

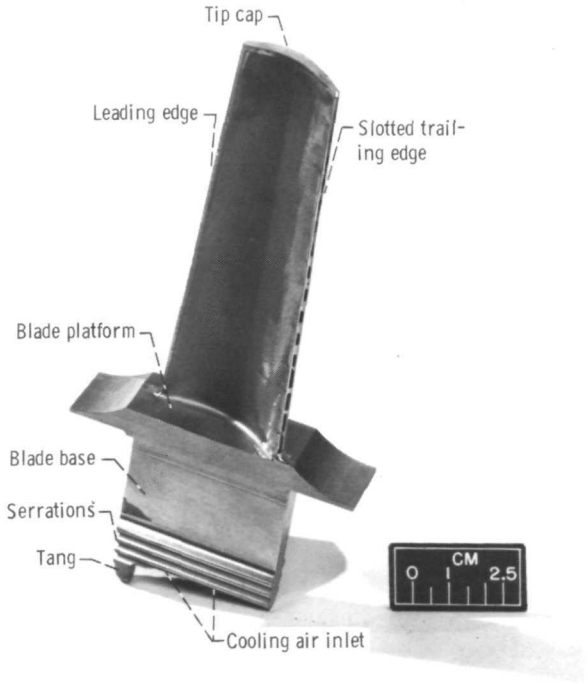

C-69-1233

Figure 7. - Chordwise-passage blade assembly.

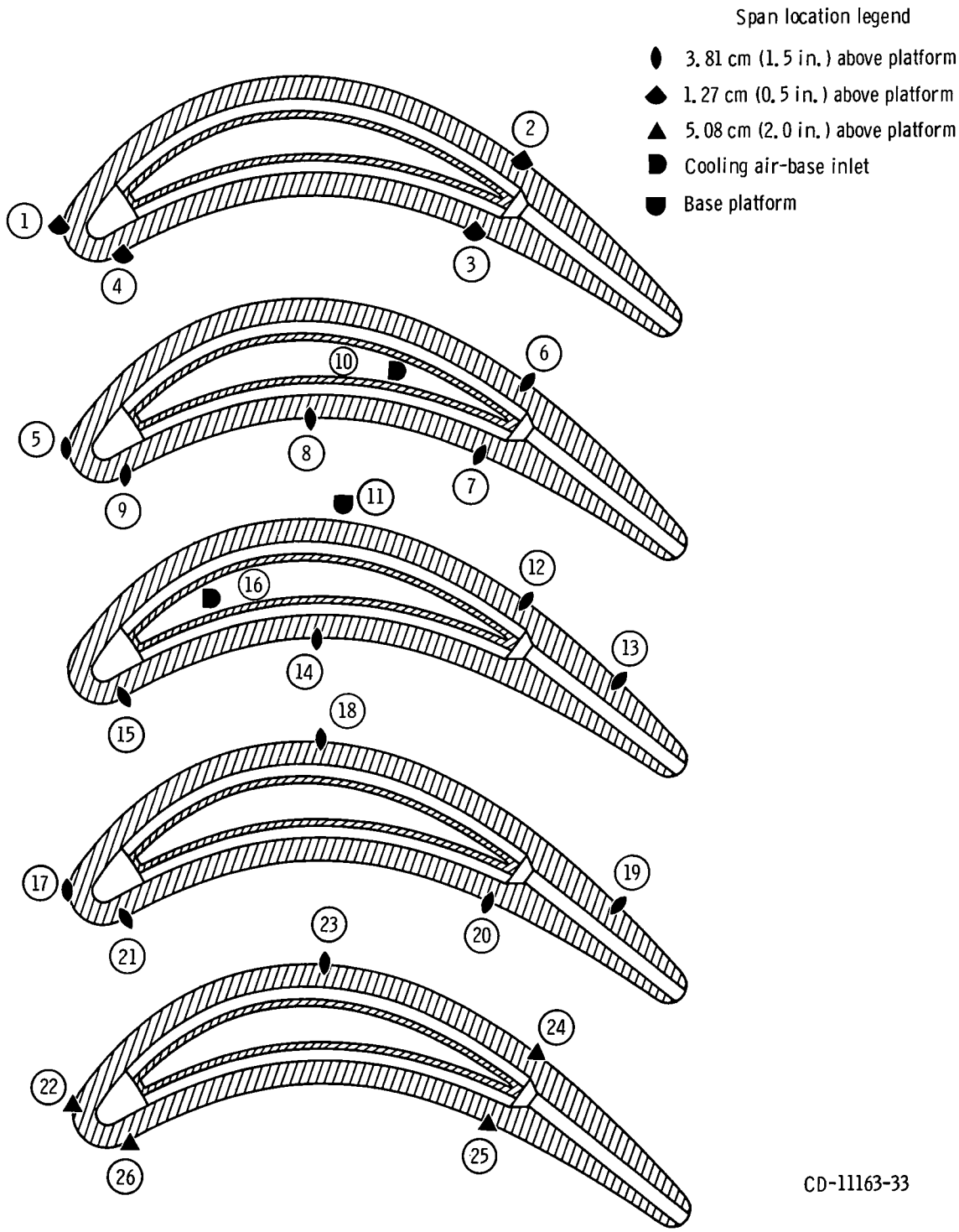

Figure 8. - Relative location of thermocouples on five adjacent test blades. Thermocouple numbers appear next to symbol location.

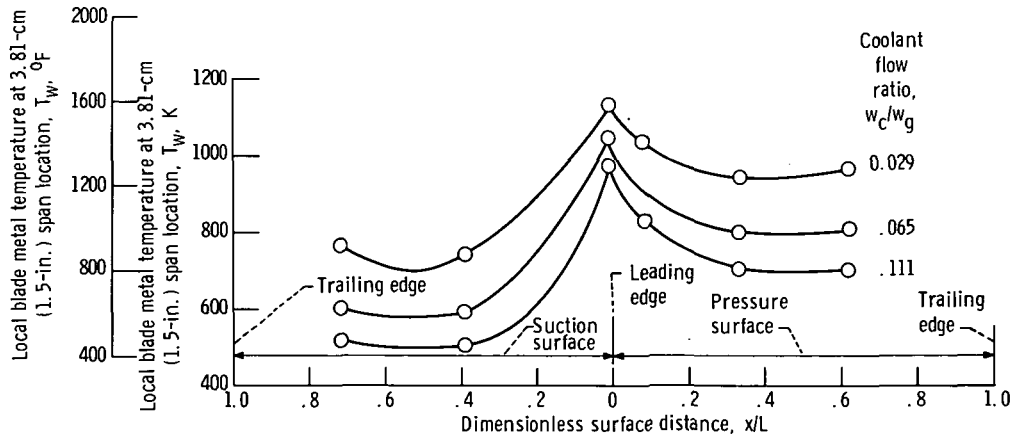

Figure 9. - Chordwise blade-wall temperature distributions for nominal relative gas temperature of 1489 K (2221^o F), nominal blade inlet coolant temperature of 361 K (190^o F), and varying coolant flow ratios.

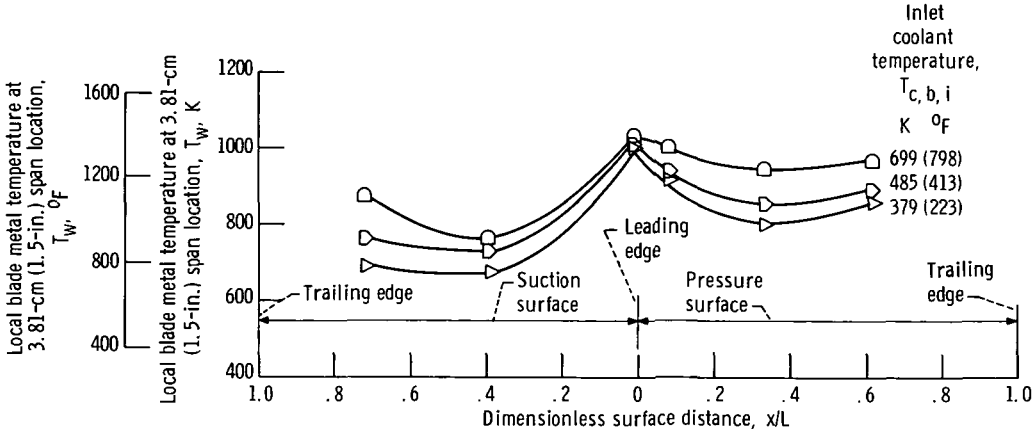

Figure 10. - Chordwise blade-metal temperature distributions for nominal relative gas temperature of 1262 K (1812^o F), a nominal coolant flow ratio of 0.03 and varying inlet coolant temperatures.

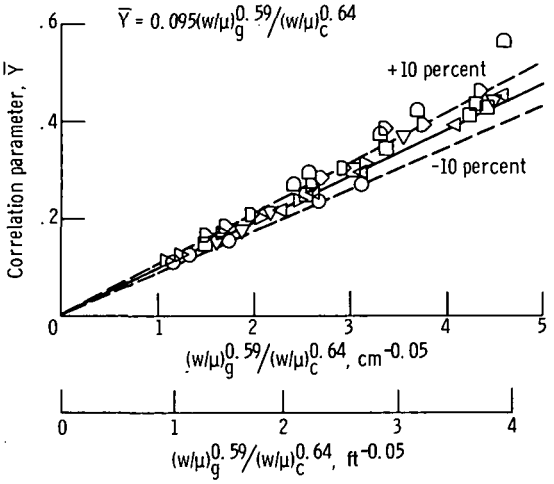

Figure 11. - Correlation of average blade wall temperatures based on equation (1).

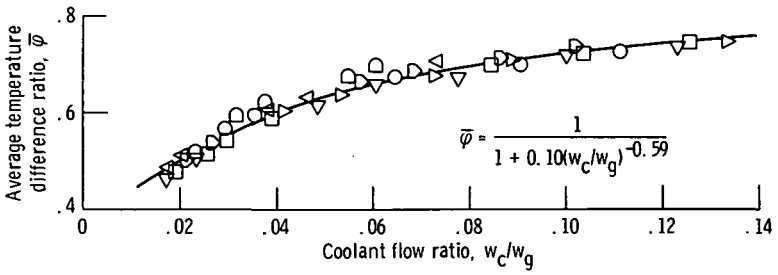

Figure 12. - Correlation of average blade wall temperatures based on equation (3).

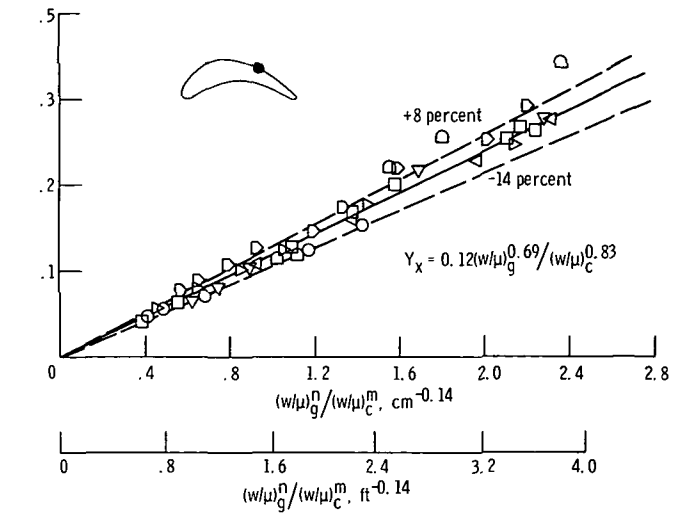

(a) Thermocouple 12.

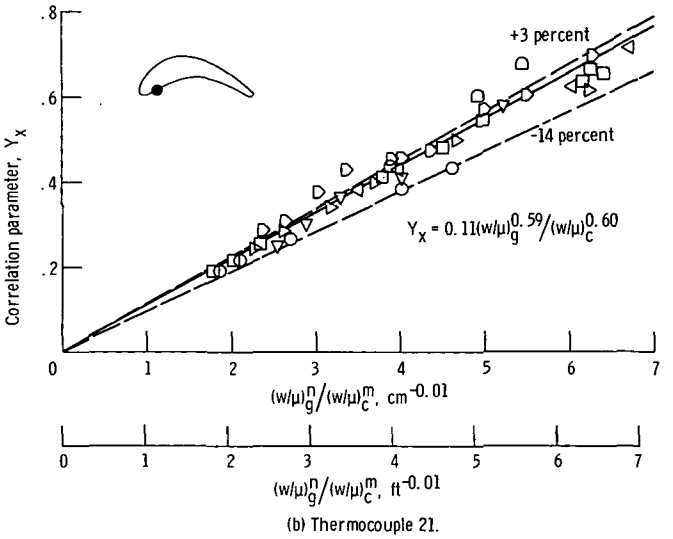

(b) Thermocouple 21.

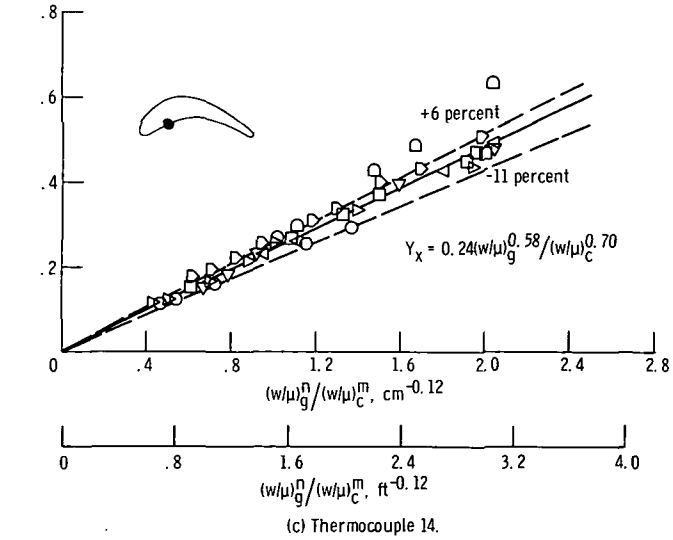

(c) Thermocouple 14.

Figure 13. - Correlation of local blade wall temperatures based on equation (1).

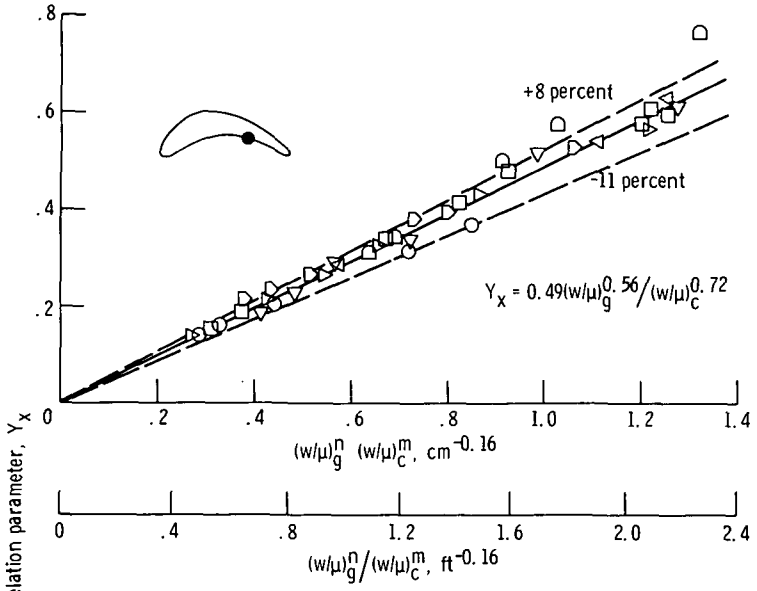

(d) Thermocouple 20.

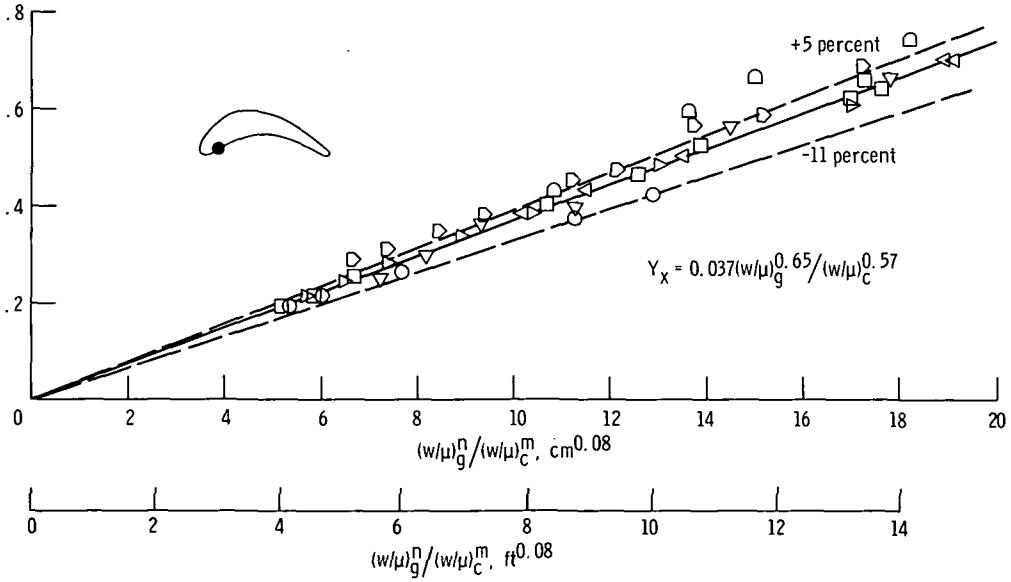

(e) Thermocouple 15.

Figure 13. - Concluded.

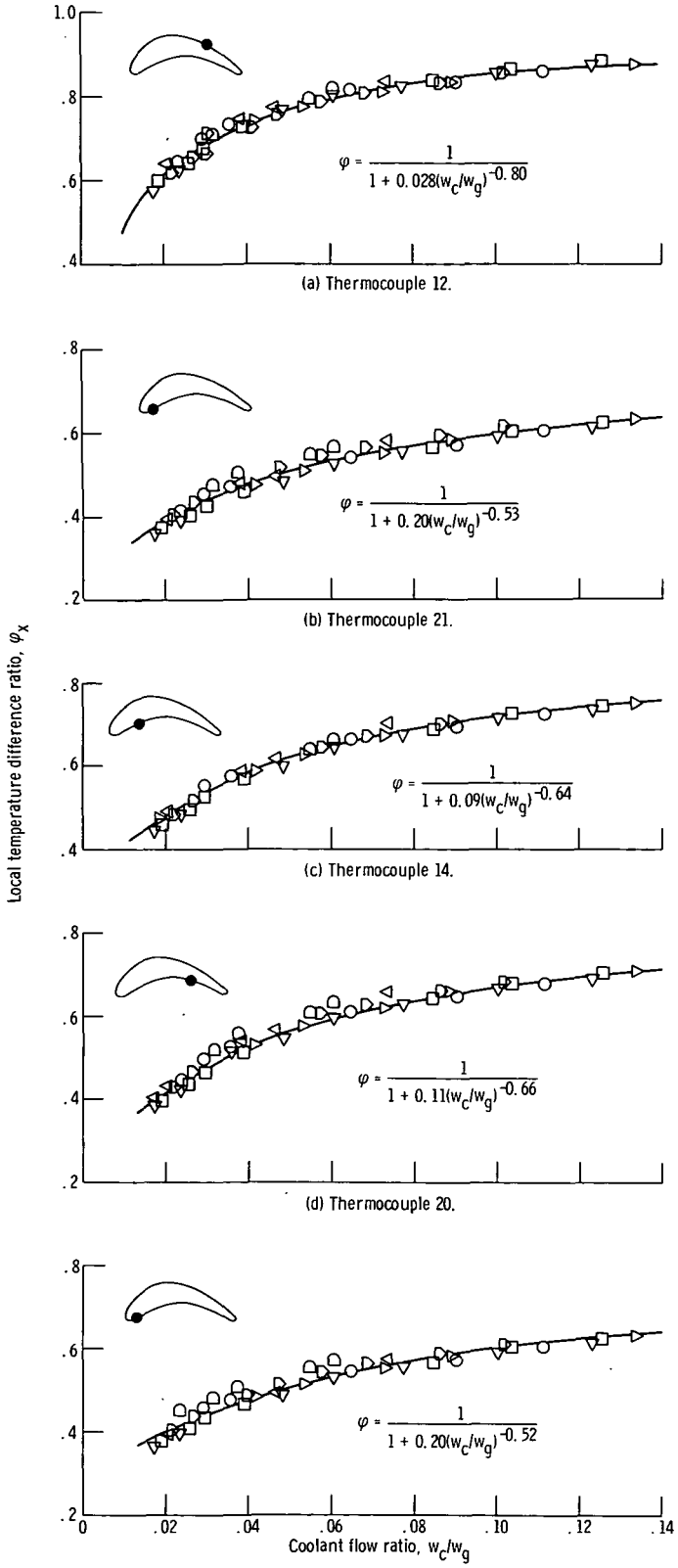

Figure 14. - Correlation of local blade wall temperatures based on φ_x correlation.

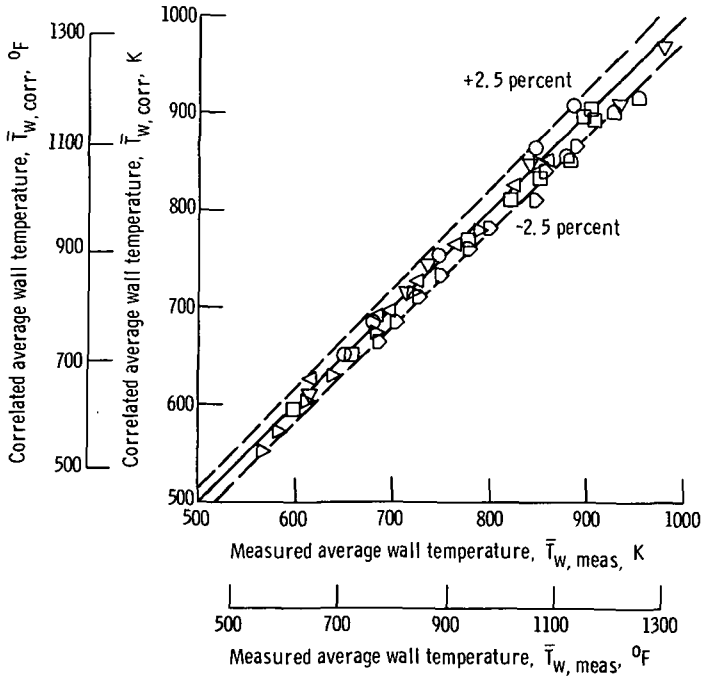

Figure 15. - Comparison of average measured blade wall temperatures with those calculated from $\bar{Y}$ correlation.

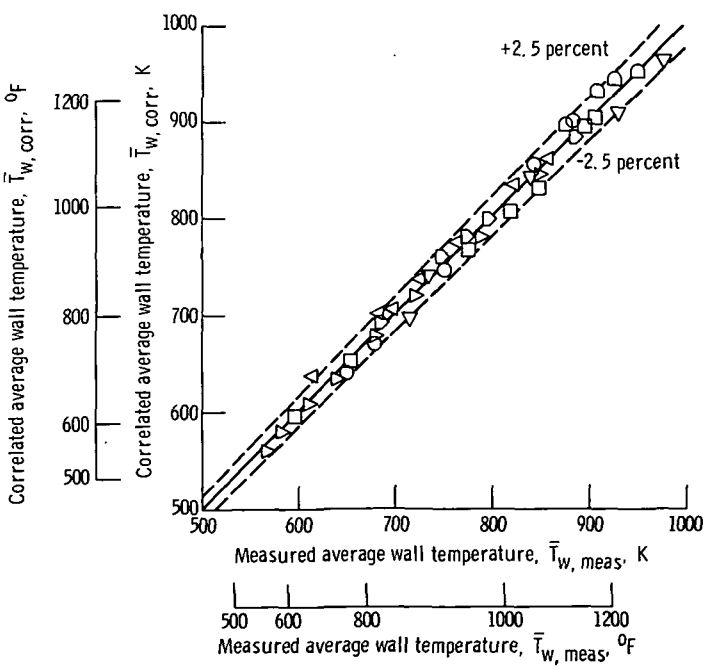

Figure 16. - Comparison of average measured blade wall temperatures with those calculated from $\bar{\varphi}$ correlation.

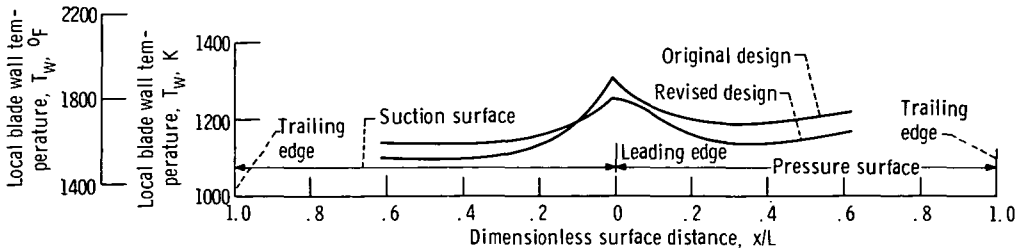

Figure 17. - Expected chordwise blade wall temperature distributions. Maximum wall temperature of 1256 K (1800^o F); relative gas temperature, 1496 K (2232^o F); coolant-inlet temperature, 922 K (1200^o F); coolant flow ratio, 0.03.

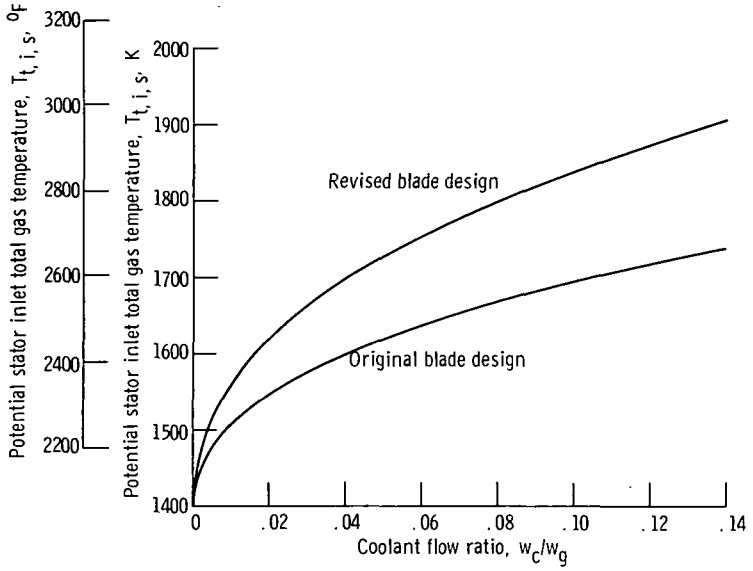

Figure 18. - Potential stator-inlet total gas temperature as function of coolant flow ratio. Maximum wall temperature, 1256 K (1800^o F); coolant-inlet temperature, 922 K (1200^o F); both original and revised blade designs.

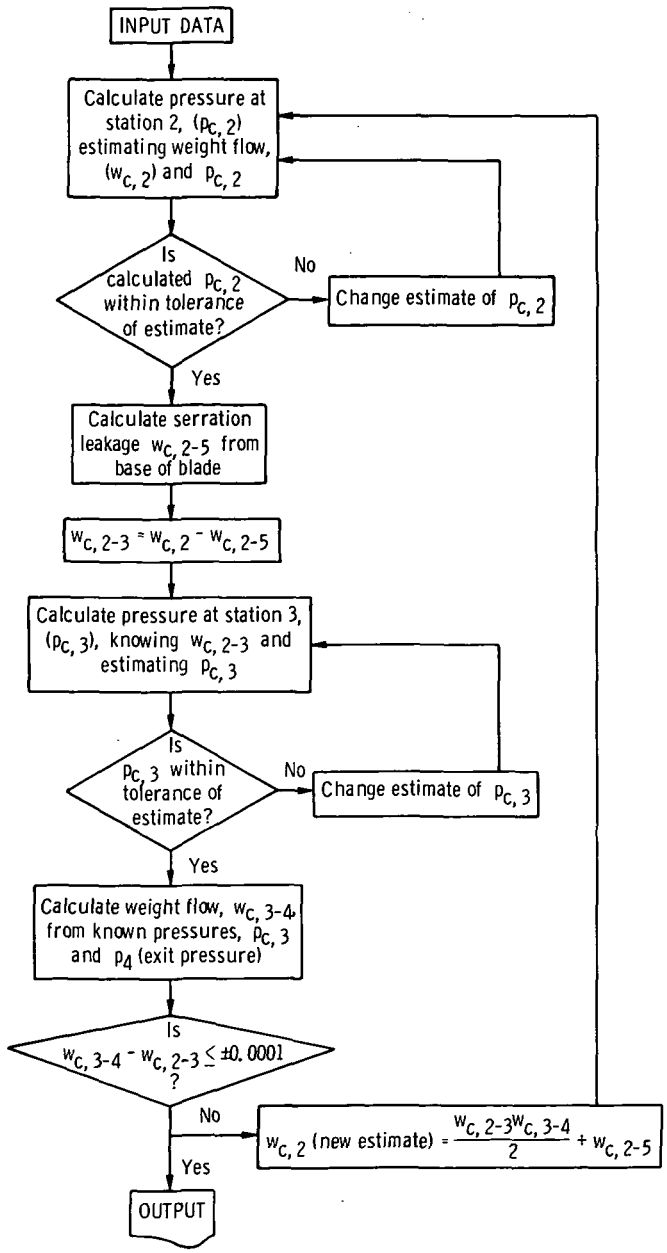

Figure 19. - Flow chart of program used to determine test blade coolant flowrate.

Page Intentionally Left Blank

NATIONAL AERONAUTICS AND SPACE ADMISTRATION
WASHINGTON, D.C. 20546

OFFICIAL BUSINESS
PENALTY FOR PRIVATE USE $300

FIRST CLASS MAIL

POSTAGE AND FEES PAID
NATIONAL AERONAUTICS AND
SPACE ADMINISTRATION

U.S.MAIL

POSTMASTER: If Undeliverable (Section 1
Postal Manual) Do Not Re

"The aeronautical and space activities of the United States shall be conducted so as to contribute . . . to the expansion of human knowledge of phenomena in the atmosphere and space. The Administration shall provide for the widest practicable and appropriate dissemination of information concerning its activities and the results thereof."

—NATIONAL AERONAUTICS AND SPACE ACT OF 1958

NASA SCIENTIFIC AND TECHNICAL PUBLICATIONS

TECHNICAL REPORTS: Scientific and technical information considered important, complete, and a lasting contribution to existing knowledge.

TECHNICAL NOTES: Information less broad in scope but nevertheless of importance as a contribution to existing knowledge.

TECHNICAL MEMORANDUMS: Information receiving limited distribution because of preliminary data, security classification, or other reasons.

CONTRACTOR REPORTS: Scientific and technical information generated under a NASA contract or grant and considered an important contribution to existing knowledge.

TECHNICAL TRANSLATIONS: Information published in a foreign language considered to merit NASA distribution in English.

SPECIAL PUBLICATIONS: Information derived from or of value to NASA activities. Publications include conference proceedings, monographs, data compilations, handbooks, sourcebooks, and special bibliographies.

TECHNOLOGY UTILIZATION PUBLICATIONS: Information on technology used by NASA that may be of particular interest in commercial and other non-aerospace applications. Publications include Tech Briefs, Technology Utilization Reports and Technology Surveys.

Details on the availability of these publications may be obtained from:

SCIENTIFIC AND TECHNICAL INFORMATION OFFICE

NATIONAL AERONAUTICS AND SPACE ADMINISTRATION

Washington, D.C. 20546